Journal of Palaeogeography
2014, 3(3): 233−256
DOI: 10.3724/SP.J.1261.2014.00054

Lithofacies palaeogeography and sedimentology

Siliciclastic−carbonate mixing modes in the river-mouth bar palaeogeography of the Upper Cretaceous Garudamangalam Sandstone (Ariyalur, India)

Subir Sarkar[1, *], Nivedita Chakraborty[1], Anudeb Mandal[1], Santanu Banerjee[2], Pradip K. Bose[1]

1. Department of Geological Sciences, Jadavpur University, Kolkata−700032, India
2. Department of Earth Sciences, Indian Institute of Technology Bombay, Powai, Mumbai−400076, India

Abstract Mixed siliciclastic−carbonate rocks constitute the Upper Cretaceous Garudamangalam Sandstone Formation, Ariyalur (India), and offer an opportunity to look into the broad spectrum of mixing of compositionally and genetically different components. The palaeogeographic reconstruction indicates that deposition in the nearshore zone differed strongly in energy and active processes operatives due to the presence of a shore-parallel river-mouth bar. The western wing of the Mississippi bird-foot delta is considered to be a present-day analogon. Facies analysis in combination with petrography clearly shows the variability in palaeoenvironmental characteristics, both biogenic and non-biogenic. It also indicates diagenetic uptake of carbonate that filled empty spaces and actively replaced original components. Chemical staining followed by limited application of cathodoluminescence and energy dispersive X-ray analysis (EDAX) hint at intricacies in mixing arising from the compositional variations in the carbonate components. A model of siliciclastic−carbonate sediment mixing, including both the depositional and diagenetic developments, is presented; it is aimed at generating a better overview of, and a deeper insight into, the physical and chemical mechanisms involved.

Key words mixed siliciclastic−carbonate succession, Garudamangalam Sandstone Formation, Upper Cretaceous, river-mouth bar, India

1 Introduction

The ultimate rock is, generally, igneous for siliciclastics and biogenic for carbonate particles. Despite this cardinal difference, both can be mechanically deposited, consequently, their depositional settings are not compartmentalized. Many modern depositional settings thus witness admixing of these two genetically-contrastive products, especially those where rivers debouch their sediments onto carbonate-depositing marine shelves (Holmes and Evans, 1963; Larsonneur *et al.*, 1982; Belperio and Searle, 1988; Larcombe and Woolfe, 1999; Dunbar and Dickens, 2003; Wright *et al.*, 2005; Ryan-Mishkin *et al.*, 2009). Mount (1984) elicited different possible modes of depositional mixing. Kidwell (1991) highlighted coquinas which are in close association with siliciclastics and added a special dimension to the spectrum of depositional mixing. Literature, nonetheless, seldom focuses upon mixing mechanisms of siliciclastic−carbonate sediments in rock records. Even rarer are studies with regard to diagenetic mechanisms of mixing. Siliciclastic and carbonate rocks are distinguished simply on the basis of relative proportions of the two compositionally-different components, no

* Corresponding author. E-mail: jugeoss@gmail.com.
Received: 2013−08−19 Accepted: 2014−01−09

matter whether they constitute the framework, matrix or cement. Replacement of primary constituents may convert a siliciclastic sediment into a limestone (Folk *et al.*, 1970).

The *ca.* 490-m-thick (Sundaram *et al.*, 2001) top part of the Mid-Upper Cretaceous Uttatur Group, Ariyalur District, India (Figure 1; Tewari *et al.*, 1998; Watkinson *et al.*, 2007), provides an excellent opportunity to enhance our insight in this matter, as it encompasses a wide range of processes that enforces depositional and diagenetic mixing between siliciclastic and carbonate sedimentary components. Facies analysis was conducted to reveal the influence of the palaeogeography on the mixing. Generally, the poor quality of exposures, because of thick alluvium cover and the general proneness of carbonate-rich rocks, often renders their sedimentary structures obliterated. The facies analysis thus had to be augmented by microscopic characterization as well. In conjunction with palaeogeography-related palaeocurrent analysis, it helps to erect a depositional model. Petrography further abets a good assessment of diagenetic introduction of carbonates. Chemical staining of thin sections and studies using cathodoluminescence (CL) and energy dispersive X-ray analysis (EDAX) refine the data regarding carbonate compositional variations evoked in the processes, biotic and abiotic. The ultimate goal of this contribution is forward modeling of mixing between siliciclastic and carbonate sediments and

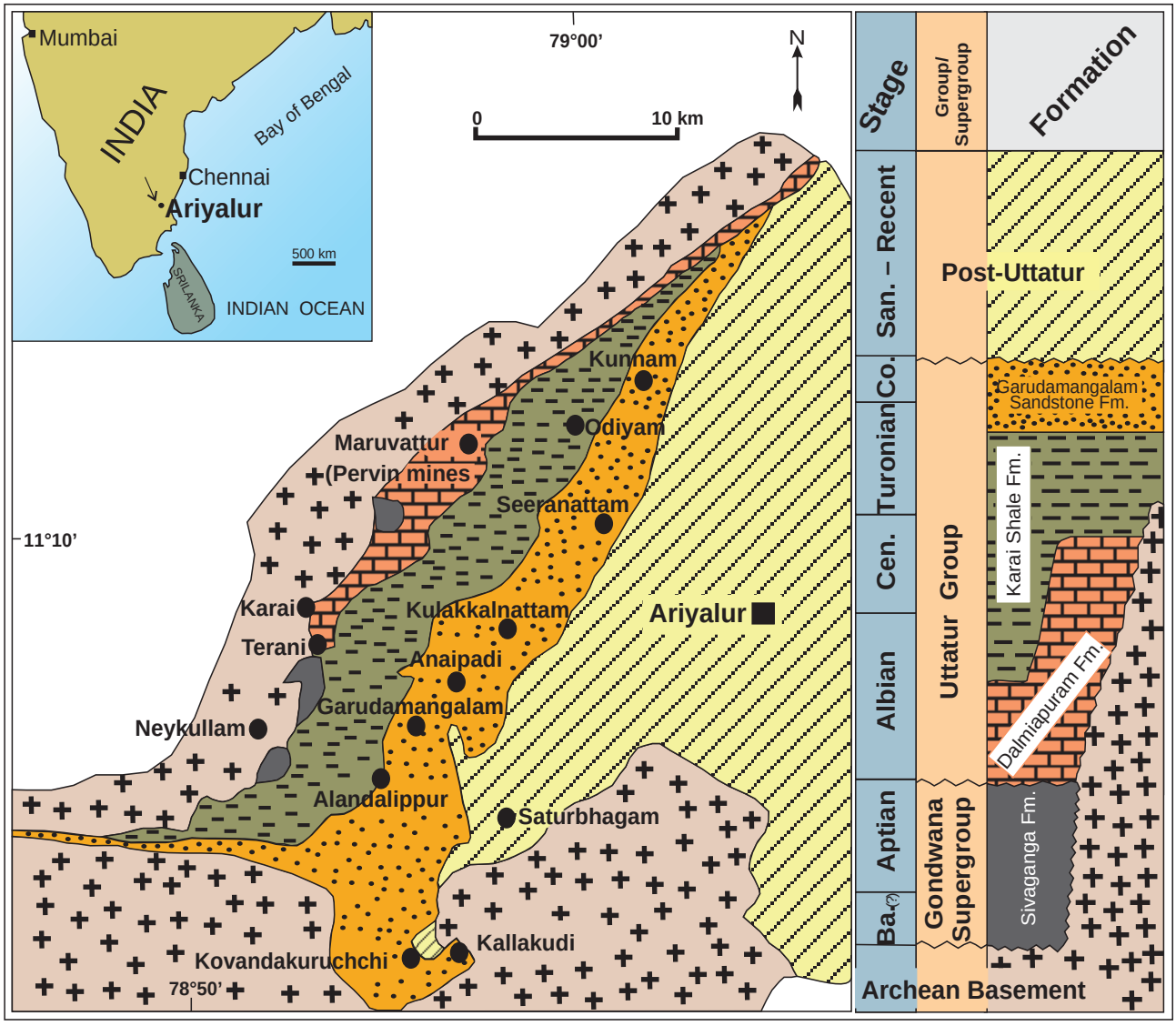

Figure 1 Geological map showing the spatial distribution of the Middle to Upper Cretaceous Uttatur Group (Dalmiapuram, Karai Shale and Garudamangalam Sandstone Formations) and post-Uttatur formations near Ariyalur (map of southern India within inset). Related stratigraphic successions are provided on the right. Note the tripartite subdivision of the Uttatur Group. Ba.=Barremian; Cen.=Cenomanian; Co.=Coniacian; San.=Santonian; Fm.=Formation.

taking into account diagenetic mixing in addition to depositional mixing. The model tees off cogitation about the pathways of such mixing in a holistic perspective.

2 Geological setting

In the Mid-Upper Cretaceous, the *ca.* 1136-m-thick Uttatur Group is exposed patchily in the Ariyalur District, India. The older basal Dalmiapuram Formation of shallow shelf origin gives way gradationally upwards into the Karai Shale Formation of deeper shelf in a transgressive trend (Tewari *et al.*, 1996; Sundaram *et al.*, 2001; Watkinson *et al.*, 2007); the latter eventually gives way upwards into the sandy Garudamangalam Sandstone Formation on account of regression (Watkinson *et al.*, 2007). In full agreement with these authors, this investigation finds the latter transition conformable, though many others placed an unconformity under the Garudamangalam Sandstone Formation and named it as the Trichinopally Group (Blanford, 1862; Ramasamy and Banerji, 1991; Govindan *et al.*, 1998; Sundaram *et al.*, 2001; Nagendra *et al.*, 2011). There is, however, no difference in opinion about the shallow marine origin of the Garudamangalam Sandstone Formation which is the main study object of the present contribution. The consensus owes much to the abundant occurrence of marine fossils of ammonites like *Romaniceras* (*Yubariceras*) *ornatissimum, Lewesicerasvaju* and *Kossmaticeras thebaldianum, Puzosia* sp., *Damesitesaff sugata*, and *Eutrephoceras* sp.; bivalves including encrusting oysters; abundant gastropod shells; brachiopods like *Pinna* and *Rhynchonellids* (Sastry *et al.*, 1968; Ayyasami and Banerji, 1984; Watkinson *et al.*, 2007); marine planktonic foraminifers and calcareous nannoplankton (Govindan *et al.*, 1996; Kale *et al.*, 2000; Watkinson *et al.*, 2007); as well as trace fossils like *Skolithos* and *Cruziana* ichnofacies represented by *Ophiomorpha nodosa, Palaeophycus tubularis, Planolites beverleyensis, Skolithos linearis, Thalassinoides suevicus, Thalassinoides horizontalis, Diplocraterion* and *Teredolites*-infested log-grounds (Hart *et al.*, 1996; Govindan *et al.*, 1998; Tewari *et al.*, 1998; Watkinson *et al.*, 2007; Nagendra *et al.*, 2010). Nevertheless, the lithological complexity, including marked lateral variations, observed within this formation remains unaccounted for within this broad shallow marine interpretation of the palaeogeography. There is no difference in opinion about termination of the Garudamangalam Sandstone Formation by a river-based unconformity on top (Tewari *et al.*, 1996; Ramkumar *et al.*, 2004; Watkinson *et al.*, 2007; Nagendra *et al.*, 2011). The Garudamangalam sandstone is thus considered as a highstand systems tract (HST). Watkinson *et al.* (2007) recognized the Anaipadi Sandstone Member, a constituent of the Garudamangalam Formation, as a HST.

3 Facies analysis

A wide spatial variability in field characteristics of the Garudamangalam Sandstone Formation is apparent (Figure 2). Notwithstanding this, limited exposures, their heavily weathered nature and extensive obliteration of internal structures hinder distinction of facies only on the basis of their field characteristics. The analysis is thus complemented with petrographic characteristics. Justification for this inclusion is that, in carbonate-rich sediments, early diagenetic alterations are commonplace, which are often controlled by depositional environments, and hence their products may compensate for the loss of sedimentary structures in palaeogeographic interpretations. Four distinctive facies associations, each with a couple of facies constituents, have been recognized within the Garudamangalam Sandstone Formation; they are described and interpreted below:

3.1 Facies association 1 (FA 1)

This is an association of medium- to coarse-grained sandstone, sometimes granular and with few skeletal fragments. Besides being remarkably poor in grain sorting, the sandstones are typically characterized by trough cross-strata (Figure 3a). One of the constituent facies (facies 1A) is distinctly coarser than the other. The cross-sets within this facies measure up to ~25 cm in thickness and are present in the frame of co-sets terminated by broadly-undulating erosion surfaces. The framework grains are generally sub-angular to sub-rounded in shape. Quartz, feldspar and biotite are the main constituents of the framework population. The feldspar grains are decomposed preferably along cleavage planes. As a consequence, many of the feldspar grains have been disintegrated into multiple fragments which extinguish together under crossed nicols. The biotite grains are commonly bleached preferably along their margins; they also have been disintegrated because of expansion across cleavage planes. Some biotite grains have been hydrolyzed and converted to greenish vermiculite. Pressure welding between framework grains is not common, but locally, resistant biotite grains are folded and pressed against harder quartz or feldspar grains. This facies also contains wood fragments with lengths of up to 81 cm (Figure 3b). This is the only facies in the studied

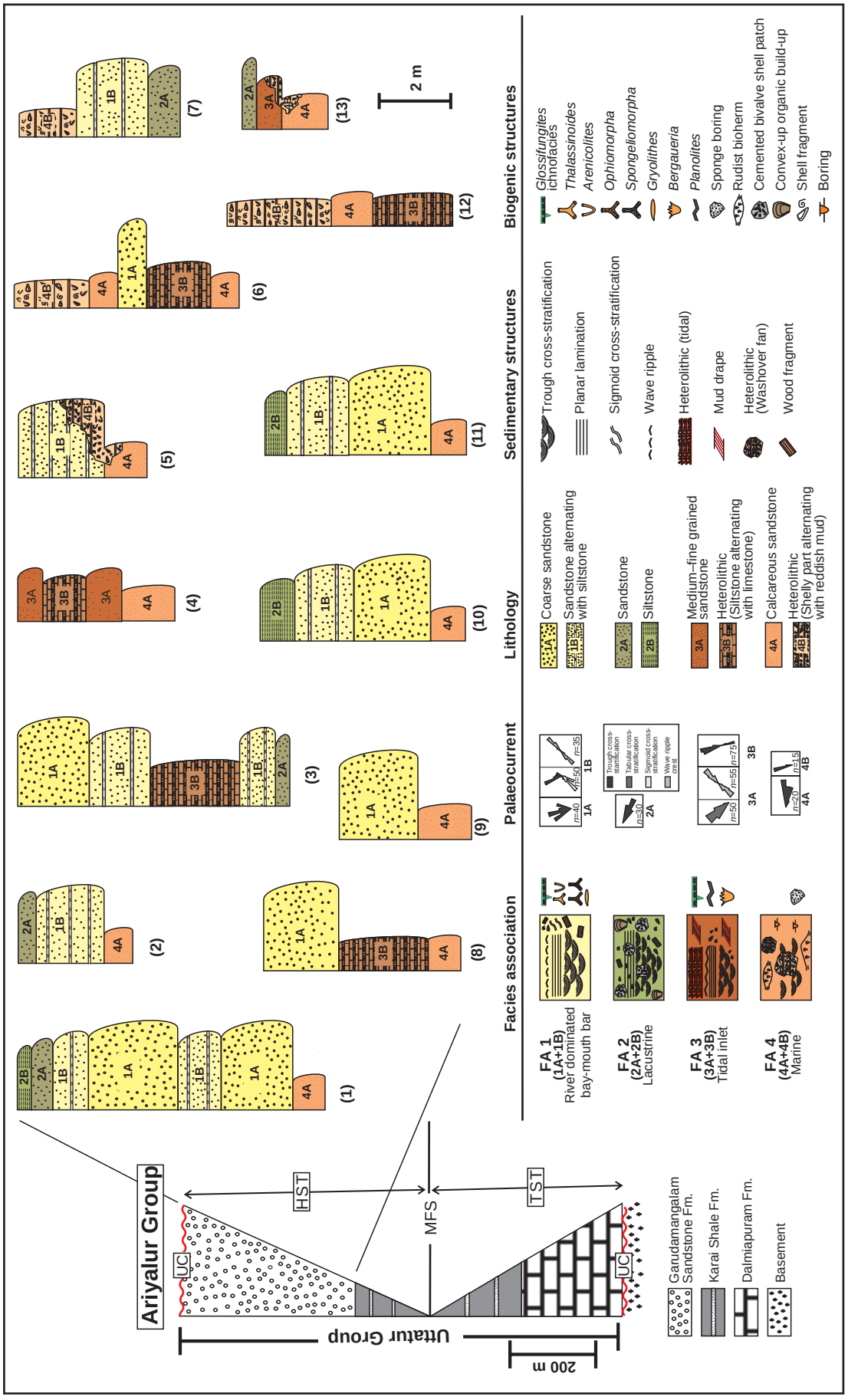

Figure 2 Deposition of the Uttatur Group bounded between two unconformities. Note the fining-upward trend in the lower part of the group while a coarsening-upward trend is present in the upper part with the presence of maximum flooding surface (MFS) in between. Four facies associations constituting the Garudamangalam Sandstone Formation are distributed over the entire area of exposure near Ariyalur. Variations in lithology, primary sedimentary and biogenic structures and palaeocurrent directions associated with the various associations are also noted. Fm.=Formation; HST=highstand systems tract; TST=transgressive systems tract; UC=unconformity.

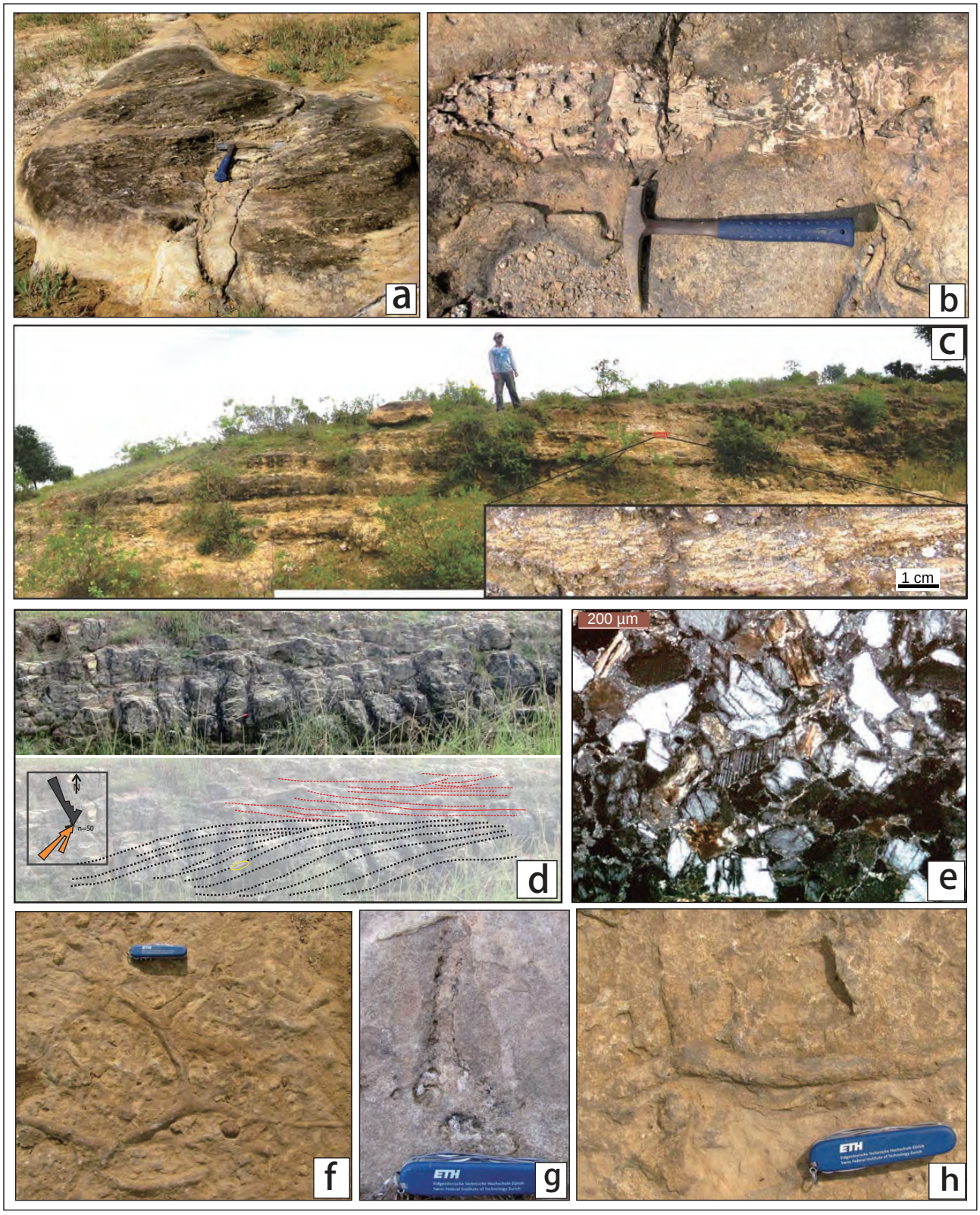

Figure 3 a−Trough cross-strata and b−A wood fragment in the coarse-grained sandstone facies 1A; c−Flat-base and convex-top sandstones with silty shale partings in facies 1B (a parting highlighted); d−Sigmoidal cross-strata within facies 1B, sketched below with significant directional variation (red rose) and associated trough cross-strata (black rose); e−Poor grain sorting in facies 1A, under crossed nicols; f, g, h−*Thalassinoides*, *Ophimorpha* and *Spongeliomorpha* traces within facies association 1. Pen (encircled in d) length=14.5 cm; Hammer length=30 cm; knife length=8.4cm; the same below.

formation which is entirely siliciclastic, but for a few specks of skeletal fragments; siliciclastic mud fills interstitial spaces among framework grains. Recrystallization of the mud matrix along the margin of framework grains is a common feature; minute grains of hydrous mica are arranged perpendicular to framework grain-surfaces.

The other facies 1B in this association is characterized by 1-m-thick sandstone beds alternating with ~6-cm-thick siltstones or silty shales (Figure 3c). Different from facies 1A, the sandstone component in facies 1B is comparatively finer grained, though still in the medium to coarse fraction and with interstitial spaces filled by calcite spar; the sandstone is calcareous. Chemical staining with alizarin red S plus potassium ferricyanide reveals a non-ferroan composition of this blocky spar. The calcite spar within the interstitial spaces looks very dirty; at places, it gives rise to sand crystals and never shows any preferred crystal arrangement around the framework grains. Set-thicknesses of trough cross-strata are also comparatively smaller, on average 12 cm. Locally there are also sets of sigmoidal cross-strata whose thickness is, however, larger, around 15 cm (Figure 3d). The latter group of cross-strata is oriented at high angles to the trough cross-strata (Figure 3d). The facies bodies, at places, have flat bases and a clear convex-up geometry (Figure 3c) and sigmoidal cross-strata are found at the flanks of these bodies. The framework composition of this sandstone is almost the same and poorly sorted as in the preceding facies (Figure 3e). The siltstone or silty shale interbeds are planar or ripple-laminated (Figure 3c).

As far as trace fossils are concerned, most of the observations come from facies 1A. The poor exposure quality, especially the lack of bedding plane exposure hindered their recognition in facies 1B. The trace fossils of association 1, as a whole, belong to the *Glossofungites* association. *Thalassinoides* (Figure 3f) and oblique *Ophimorpha* (Figure 3g) are common in both facies. There are also suspected *Arenicolites* in facies 1A and *Spongeliomorpha* (Figure 3h) in facies 1B.

Interpretation

The general poor grain sorting (Figure 3e) with distinct bimodality between the framework and matrix populations and ubiquitous trough cross-strata (Figure 3a) with unidirectional orientation strongly suggest fluvial influence in the deposits of facies association 1 (Figure 2). Calcite spar having a dirty look suggest primary filling of the grain interstices by siliciclastic mud in case of facies 1B too; the abundant occurrence of sand crystals suggests slow replacement by carbonate because of a low ionic concentration in the pore water (Pettijohn, 1975). All these as well as the blocky nature of the spar are consistent, though not unequivocally, with fresh water influence (Bathurst, 1975; Tucker, 1981). The non-ferroan composition of the blocky spar is also consistent with the supposed shallowness of the depositional site readily entering into an oxidizing vadose zone during diagenesis. The presence of wood fragments further corroborates ready access to land materials. Nonetheless, the type of burrows present a clear evidence of deposition in the marine realm, resembling those of modern bay-mouth bars. Reconciling fluvial and marine influences, the depositional environment appears to be tied-up with a river-dominated deltaic bar (*e.g.*, van Heerden and Roberts, 1988; Pearson and Gingras, 2006). By grain sorting and primary structures, facies 1A closely resembles river channel deposits (Cant and Walker, 1978; Fielding, 1986; Miall, 1996; Gibling, 2006), while facies 1B with relatively better exposure quality facilitates recognition of a bar form. While the trough cross-strata indicate the direction of migration, the sigmoidal cross-strata indicate the direction of accretion of the bar (Chaudhuri and Howard, 1985). The siltstone interbeds in the latter facies were possibly deposited in sheltered interbar regions. The uncompacted circular cross-sections of *Thalassinoides* bear clear evidence of early cementation of the host sandstones. The carbonate spar replaces the siliciclastic matrix within grain interstices, thus appearing to be early diagenetic and be formed under the diluting effect of river water on Ca^{2+} and HCO_3^{2-} ionic concentration. Facies 1B, for its comparatively finer framework elements, appears to have deposited away from the main supply route of fluvial sediments. The early carbonate cementation and the presence of *Gyrolithes* are well consistent with a sheltered environment (Dworschak and Rodrigues, 1997) characterized by a higher than normal marine salinity (Buatois and Mángano, 2011). Facies 1B is thus interpreted to be deposited on the bayward flank of a river mouth bar.

3.2 Facies association 2 (FA 2)

This facies association is made up of very fine-grained sandstone and siltstone in which the groundmass consists of carbonate mud. The massive but relatively better exposed sandstone facies 2A often shows trough cosets, with thicknesses of the individual cross-sets of up to 11 cm. Similar to facies 1A, this facies also contains wood fragments as long as 10 cm. Locally there grow organic patches of indeterminate origin, with some like convex-up stromatolites (Figure 4a), and some as irregular patches of thick-cemented shells of sedentary bivalves. In thin

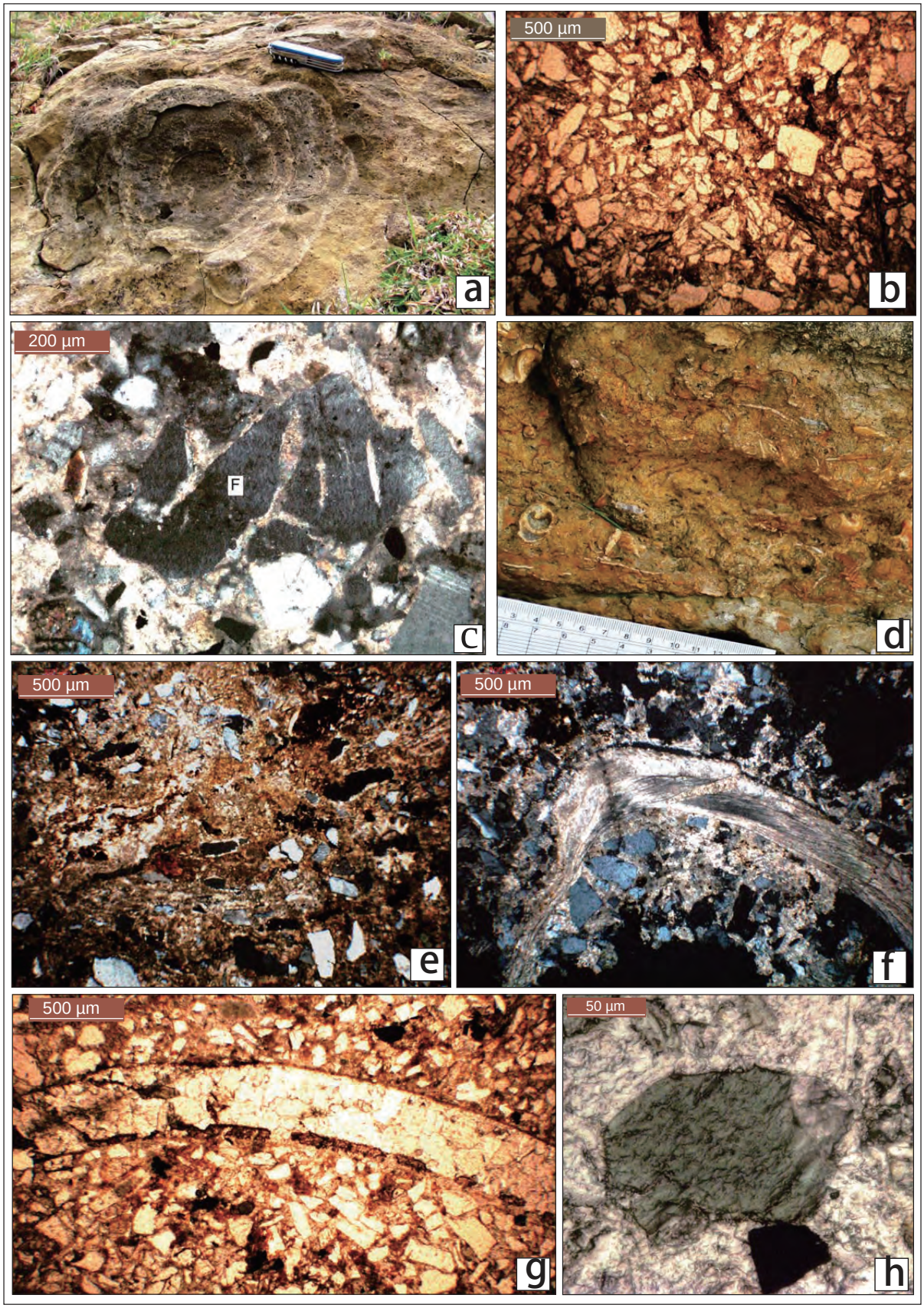

Figure 4 a−A stromatolite-like convex-up biogenic build-up; b−Moderately sorted texture; and c−Carbonate-replaced feldspars (F) along cleavage planes, in facies 2A; d−Reddish siltstone enriched in skeletal grains; e−Minuscule red algae growth; f−An *Ostrea* shell with inherited fabric; g−A bivalve mould with micritized rim; and h−Glauconitized feldspar as well as pyrite, within facies 2B.

section, its framework grains include quartz, feldspar and mica, moderately sorted (Figure 4b) and often bleached. The quartz and feldspar grains are sub-angular to sub-rounded in shape. The feldspar grains are usually fresh but replaced by carbonates along cleavage planes (Figure 4c); while quartz grains are also nibbled at their margins. Specks of glauconite are present, some of which are evidently derived from potash feldspar and biotite. The few bivalve clasts present are made of non-ferroan calcite and preserve their primary fibrous texture. The interstitial spaces between grains are filled by lightly iron-stained non-ferroan carbonate mud, locally recrystallized to microspar. Some isolated specks of opaque grains of pyrite occur scattered within the groundmass.

The other constituent facies 2B of this association is a massive reddish siltstone (Figure 4d). Skeletal grains are present sparingly, but in higher frequency than in facies 2A. Under a microscope the rock appears to be made of well-sorted silt-sized siliciclastic grains almost floating within non-ferroan carbonate mud, deeply stained in iron. At places, however, there are siliciclastic sand-sized grains, clearly over-sized with respect to the general framework population. The siliciclastic population is composed of quartz and feldspar; mica is virtually absent. All the siliciclastic grains are angular and with ferruginous coatings. Specks of deep red iron cement also float within the carbonate groundmass. The carbonate groundmass locally displays minute steep convex-up biogenic growth structures possibly of red algae (Figure 4e; Cornée *et al.*, 2012). There are also a few minute drum-shaped biotic fragments, possibly of microbial origin. Some curved shells are present in comparatively greater abundance; some of them retain their primary fibrous textures, others do not; some of the former group of shells belong to *Ostrea* (Figure 4f). The skeletal population also includes some species of forams. Non-ferroan calcite constitutes both the preserved shells and the moldic pore cements. Micritic rims are present on many shells, preserved or dissolved (Figure 4g). The rims are, however, made of ferroan calcite, at least, partially. Glauconite is present in relatively greater abundance than in facies 2A, and again its origin can be traced to potash feldspar, at least, in some cases. Small specks of pyrite are also present, preferably within the clusters of glauconite (Figure 4h).

Poor exposure conditions prevented any assessment regarding bioturbation. It is certain, nevertheless, that burrowing activities had been very limited. As for trail marks, the complete absence of any bedding plane exposure prevented their recognition.

Interpretation

The skeletal and trace fossils as well as the carbonate groundmass jointly suggest marine influence in the depositional environment. The presence of authigenic glauconite supports this contention. Deposition apparently took place in a considerably low energy regime where the rate of sedimentation was low and amenable to chemical precipitation. Skeletal and microbial mounds, though often in miniscule dimensions, support this contention. However, the frequent presence of wood fragments suggests shallow water deposition, perhaps in a sheltered place. The scarcity of fossils and burrows has a high preservation potential in early-cemented carbonate-rich sediments, and supports the contention that the depositional environment had been restricted and hostile like a bay or a lagoon. Differential dissolution of shells in facies 2B evinces a difference in primary mineralogy (Bathurst, 1975; Morse and Mackenzie, 1990). Presumably the aragonitic shells dissolved preferentially, but retained their shapes because of early cementation of the sediments hosting them. The non-ferroan nature of the entire calcitic groundmass, *i.e.*, the primary grains and the cements within their interstices, suggests oxidizing conditions that prevailed during this early diagenesis. The same oxidizing conditions continued during filling of moldic pores probably in the vadose zone; the blocky nature of the cement crystals suggests influence of meteoric water. The water that caused shell dissolution likely maintained saturation with respect to calcite discriminating against aragonitic shells and sparing those with calcitic mineralogy (Morse and Mackenzie, 1990). Partial replacement of micritic calcite rims of possible marine phreatic diagenetic origin formed around the shells by ferroan calcite is likely to have taken place during subsequent burial; other calcite crystals, primary or secondary, escaped because of, inter alia *inter alia*, their larger size. Complete elimination of aragonite beforehand possibly prevented the smallest calcite crystals to escape the transformation. The ferroan composition of the new crystals is due to presence of iron with a comparatively smaller ionic radius in the ferrous state. Glauconitization, nonetheless, indicates turning of the diagenetic environment to dysoxic conditions, even at an early stage. Pyritization, mostly consuming the iron from the early diagenetic glauconite, bears testimony to the establishment of an anoxic state during burial.

Because of the distinctly finer size of the siliciclastic grains, the depositional site of facies 2B is interpreted to be further away from the depocenter than facies 2A. The carbonate groundmass containing biotic particles and biogenic growth structures in the former is apparently indig-

enous. The floating fabric of the silt population within the carbonate groundmass in facies 2B may owe its origin to intense bioturbation; but in absence of any "swirl" texture, the probability is low. More likely is an allogenic origin of the population; the good sorting, freshness of feldspar grains, ferruginous coating and sharp angularity of grains suggest an eolian loess origin of the silt population. Presence of a few distinctly over-sized sand grains locally within this calcareous siltstone or silty limestone possibly indicates the transitional zone between the two facies; the sand grains having spilled from the deltaic mouth bar. The stressful nature of the restricted depositional setting accounts for the failure to present a credible trace fossil record and ensured microbial mat growth. Disseminated pyrite crystals are consistent with the depositional setting envisaged. Deposition presumably took place in the behind-bar embayment.

3.3 Facies association 3 (FA 3)

This facies association consists of a medium- to fine-grained moderately-sorted sandstone facies 3A and a heterolithic facies 3B, with contrasting framework compositions, *viz*. siliciclastic and calcareous, respectively. Sandstone facies 3A is generally characterized by cross-strata, planar at places and troughs elsewhere. Dune-like bedforms with an average height of 42 cm are often well exhumed on bed surfaces. A substantial shell concentration at the toe is typical of these bedforms (Figure 5a). The internal cross-sets often display well-defined mud drapes. Another difference with facies 3A is the near-absence of mica and fresh feldspar grains, even though nibbled by carbonate at their margins or replaced along cleavage planes (Figure 5b). The sand population of this facies is constituted mostly by quartz and feldspar as well as skeletal material, though with restricted distribution, at bedform toes.

Framework elements in facies 3A are often found detached from each other and floating within the carbonate groundmass; however, unlike that in facies association 2, this groundmass is made of blocky calcite crystals, none of which appear to grow with support from grain walls. There is no drusy growth within grain interstices. At places, the carbonate crystals form large sand crystals embedding multiple sand grains (Figure 5c; Pettijohn, 1975). These carbonate crystals are generally dirty in appearance and at places contain minute relict particles (Figure 5d). Non-ferroan calcite cement fills the moldic pores while ferroan calcite is more frequent within intraparticle pores. However, secondary ferroan calcite may surround the non-ferroan calcite cement. At places, pyrite crystals occur at the center of such pores. Glauconite grains, both fresh and oxidized, are locally present.

The other facies (3B) has two distinct subfacies, siltstone (Figure 5e) and limestone (Figure 5f), with the latter in dominance of carbonate skeletal material. Alternating repeatedly between themselves, interstitial spaces are filled by non-ferroan blocky carbonate crystals in both cases.

The first subfacies, the siltstone, is well sorted and with considerably thinner bodies in contrast to facies 2B, not exceeding 6−7 cm. It is impoverished in mica grains as well as shell fragments. Internally it is cross-stratified or planar-laminated, but it may also be massive (Figure 5e). However, framework grains here also float within the carbonate groundmass made of blocky calcite, often giving rise to sand crystals and never seen to grow with grain-wall support. The carbonate crystals are also dirty and contain relict grains. Also at places some relict structures run across individual calcite crystals. Quartz and feldspar, looking fresh, constitute almost the entire bulk of the siliciclastic population. Both quartz and feldspar grains have nibbled margins but feldspar grains are preferably replaced by carbonates along cleavage planes. Glauconite pellets are both fresh and oxidized.

The other subfacies, the limestone, is very rich in shell fragments and profoundly cross-stratified (Figure 5f). The shells concentrate preferably along bases of normally graded foresets that are characteristically draped by reddish mud. The foresets are on average 4 cm thick, while the mud drapes are much thinner and contain few shell fragments (Figure 5f). There are a few vertical burrows around 3 cm in diameter and 15 cm in length with their boundaries mostly fuzzy. The burrow-fills are characterized by sand-mud alternations and unlike their host sediments, virtually shell-free. In the lower part of the foresets, the skeletal fragments are mixed with fine silt-sized quartz and feldspar. The grains interstices are filled by carbonate groundmass made of blocky non-ferroan calcite which, as in the previous cases, neither give rise to drusy growth, nor appear to have taken grain-wall support while growing. The same silt fraction is also present within the mud drapes, but in association with a substantial amount of mica and less as well as smaller skeletal fragment (Figure 5g). The feldspar grains are characteristically fresh in nature. Both quartz and feldspar grains are nibbled and replaced by carbonate along their margins. Carbonate replacement has also taken place along the cleavage planes of the feldspar. In the muddy top part of the foresets carbonate cement is hardly recognizable as the interstitial spaces are

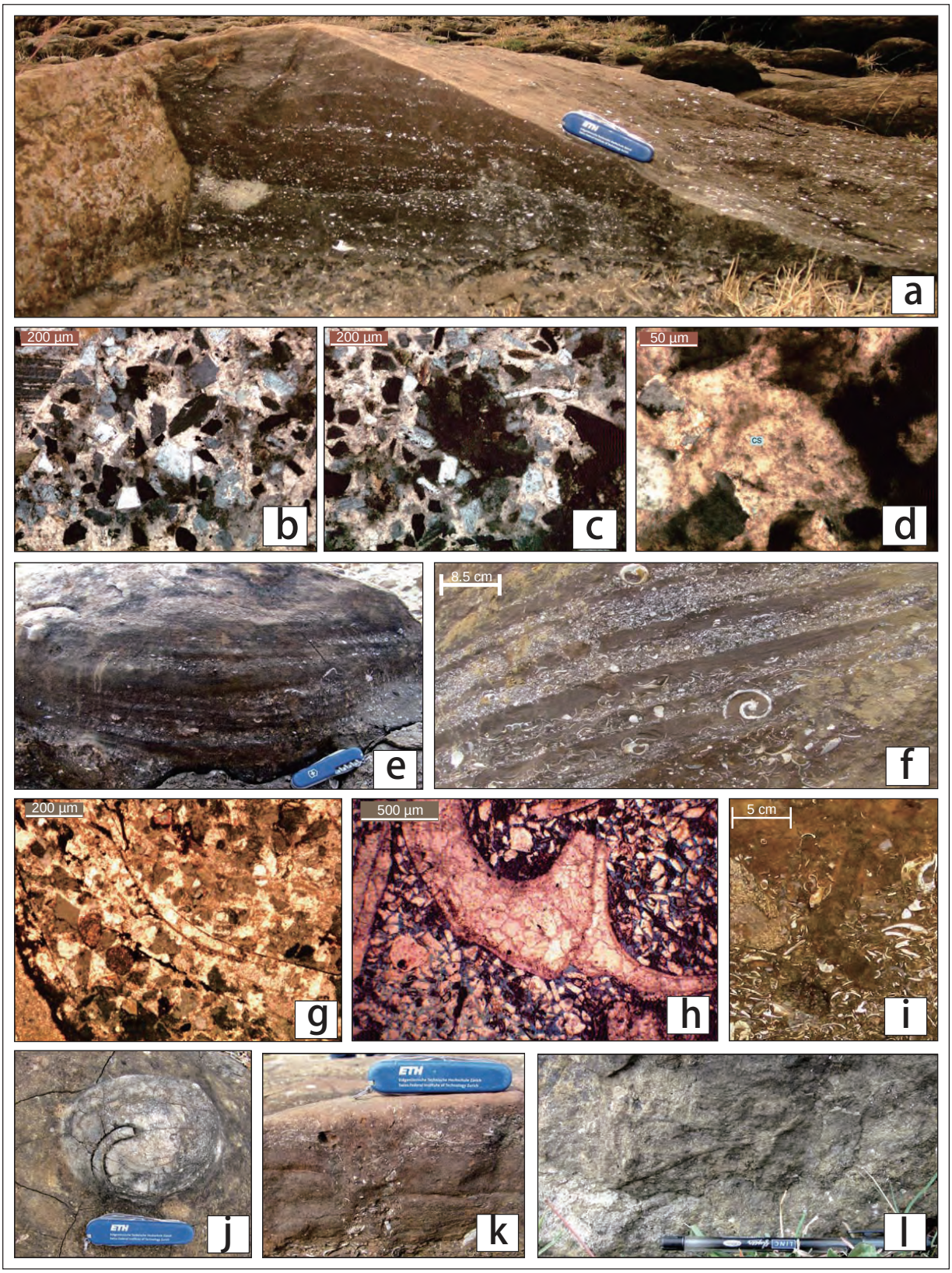

Figure 5 In facies 3A, a−A dune-like bedform with shell concentration at toe; b−Nibbling of siliciclastic grains along their margins and along cleavage planes by carbonate; c−Large extinguished sand crystal; d−Dirty carbonate with relict particles within interstices. In facies 3B, e−A planar laminated siltstone; f−A shell-rich limestone having foresets draped by mud; g−Silt and skeletal fragments within mud drapes; h−Intercrystalline pores are filled by ferroan calcite; Burrows in this facies association: i−*Glossifungites*; j−*Planolites*; k−*Bergaueria*; l−*Gyrolithes*.

filled by reddish coloured mud. The skeletal grains are mostly of curved shells, echinoid plates and spines. Some skeletal materials retain their primary fabric, others do not, but the calcite in all of them is non-ferroan, although micritic rim around them is ferroan. In the former group, however, intercrystalline pores are filled by ferroan calcite (Figure 5h). Drusy growth of clear ferroan calcite crystals is present only within some moldic pores.

The trace fossil assemblage clearly points to the *Glossifungites* ichnofacies (Figure 5i), and includes *Planolites* (Figure 5j), *Bergaueria* (Figure 5k) and *Gyrolithes* (Figure 5l). A monospecific tendency is apparent within it.

Interpretation

The ubiquitous presence of mud drapes indicates that this facies association was tide affected (Terwindt, 1988). The tidal effect is also recorded in mm-scale sand−mud alternations within the burrow-fills (Longhitano and Nemec, 2005; Pearson and Gingras, 2006; Gingras *et al.*, 2012). The fossils and trace fossils leave no doubt about deposition in a marine environment. The monospecific tendency in the trace fossil assemblage points to a stressful depositional environment. On the other hand, the micritized rims of skeletal material also indicate deposition within the photic zone. The generally good sorting of the siliciclastic material and the carbonate groundmass are consistent with the shallow marine depositional setting ensuring repeated sediment reworking. The comparatively finer grain size puts the association in a relatively lower energy regime with respect to the preceding river mouth-bar association. The burrow abundance also points to a site of deposition generally low in energy. In support of the latter, important arguments are the lack of burrows in the sandstones of the heterolithic facies, a high flow regime product with internal massiveness or planar lamination, in contrast to the abundance of burrows in the alternating limestones. Considering all these aspects, a tidal inlet origin for this facies association is interpreted. Facies 3A being relatively coarser and poorer in mica content originated in the thalweg of the tidal inlets whereas facies 3B on or close to their banks.

The retention of the primary shapes of dissolved shells evinces early cementation of the surrounding sediments. The dirty appearance and presence of abundant impurities within the blocky calcite crystals filling the grain-interstices suggest replacement of the carbonate groundmass. Their non-ferroan composition suggests precipitation under oxidizing conditions, in a shallow marine domain. The sand crystals point at slow growth of these large calcite crystals incorporating multiple sand grains and thereby attest to dilution of pore water by the influx of meteoric water. The non-ferroan nature of the calcite crystals in the groundmass as well as within the moldic pores suggests oxidizing conditions during a large part of the diagenetic history of the sediment. This contention is further supported by the ferroan composition of the calcite crystals filling the intercrystalline pores within unaltered shells as well as within the carbonate groundmass. Within the unaltered shells, decomposition of organic tissues presumably generated the intercrystalline pores and could have created reducing microenvironments to facilitate the incorporation of Fe^{2+} within the newly precipitated calcite, so that there is no need to evoke burial diagenesis to explain ferroan nature of the cement crystals. The ferroan intercrystalline pore-filling cement within the groundmass is, nonetheless, the definite product of burial diagenesis with a severely depleted supply of oxygen (Grover and Read, 1983; Niemann and Read, 1988; Kaufmann, 1997; Meyers, 1991). However, the ferroan composition of micritic cements on the shells is enigmatic because the cement is presumed to have grown right on the seafloor (Machel, 2000). Possibly, the crystals constituting the rims underwent selective replacement during burial diagenesis because of their micritic size (Choquette and James, 1987; Pirrie *et al.*, 1994).

3.4 Facies association 4 (FA 4)

This facies association is characterized primarily by well-sorted calcareous sandstone with locally intense bioturbation and patchy build-ups of rudist bivalves (facies 4A; Figure 6a). The only current structure that can, locally, still visible are trough cross-sets that are up to 10 cm thick. Some bed surfaces bear numerous polygonal cracks as well as minute borings (Figure 6b). Because of the frequent presence of highly bioturbated patches (Figure 6a) and large shell fragments, exposures of the facies are intensely weathered and consequently current structures are generally obliterated. Small bioherms of rudists are locally present within this calcareous sandstone (Figure 6c). Besides, it also includes a facies of heterolithic nature (facies 4B), present in small isolated patches, apparently similar to the limestone component of facies 3B. The sandstone (facies 4A) is medium-grained, moderate- to well-sorted (Figure 6d). The framework population in this facies includes quartz, feldspar and numerous skeletal fossils, and is almost entirely devoid of detrital mica. The majority of the siliciclastic grains are sub-rounded. Feldspars are generally fresh but may be replaced by calcite along margins and cleavage planes. Small blebs of glauconite are present in fairly high frequency (Figure 6e). There are feldspar

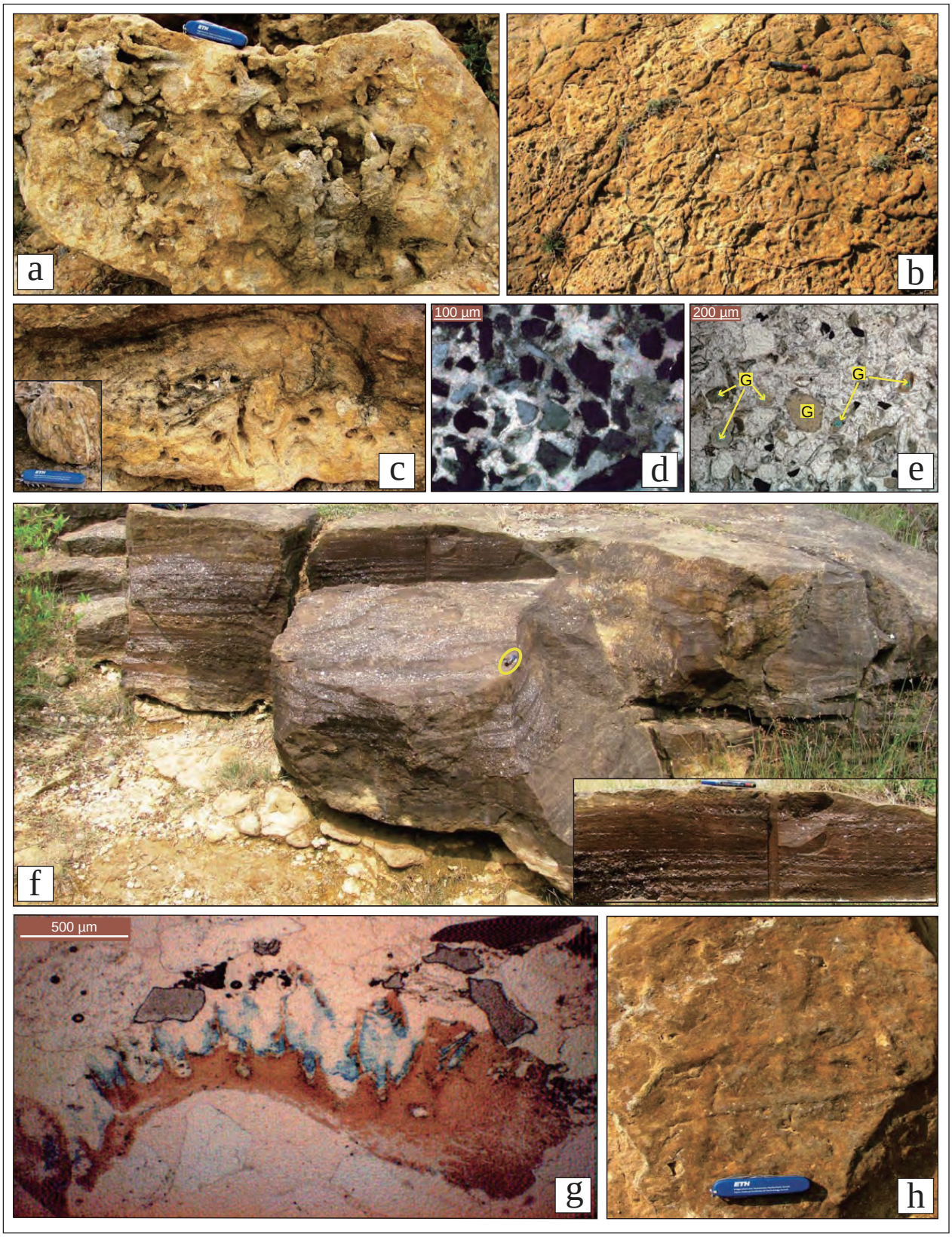

Figure 6 a−Intense bioturbation in certain beds; b−Polygonal cracks in a burrowed bed; c−Rudist bioherm and columnar shells within inset; d−Good sorting in framework elements and carbonate groundmass; e−Authigenic glauconite (G); f−Low angle cross-laminae constituted by coupled shell-rich and mud laminae (highlighted within inset) in facies 4B; g−Fabric-controlled dissolution of shells in facies 4A; h−Abundant *Thalassinoides* within the association.

grains which are glauconitized to a variable degree. The interstitial spaces between framework elements are filled by clear blocky non-ferroan calcite spar. Drusy growth is absent within intergranular pores; the crystals do not avail themselves of grain-wall support and sand crystals are conspicuous in absence. The framework elements often float within carbonate groundmass. The majority of skeletal material generally retains pristine texture. The skeletal calcite crystals are also almost without exception non-ferroan in composition; ferroan calcite, however, occurs within small dissolution cavities. The distribution of the dissolution cavities is often controlled by the primary fabric of shells (Figure 6g). Ferroan calcite also occurs along growth lines of some shells and fills the intercrystalline spaces, preferably on the outer side of shells and also in parts of the micritic rims around shells.

The heterolithic facies (facies 4B) comprises a stack of lower shelly beds and upper nearly shell-free reddish muddy beds, and has been found only in small patches not exceeding 3 m in lateral extent and 1.5 m in thickness (Figure 6f). In its best exposure, it is found to fill a sag, presumably erosional, within a rudist bioherm. The facies body has a concave-up base and a slightly convex-up top. Internally being characterized by repeated alternations between thicker shell-rich beds and thinner reddish mud beds (Figure 6f), this facies has an apparent similarity, as mentioned before, with the limestones in facies 3B. Differences, at a smaller scale, are significant: (1) The layering is, more or less, horizontal or, occasionally, with a low angle; (2) The shell bands have a somewhat irregular geometry because of lateral pinching and swelling; (3) The swelling can, at places, be related to load casts present at the base of shelly beds; (4) Concave-up and convex-up shells occur in comparable frequency; (5) Locally normal grading is discernible in these beds; (6) In that case, a depositional continuum is depicted between the lower shelly beds and the mudstone beds overlying them; (7) The mud beds are reddish in colour, and internally massive; (8) The two rock types together give rise to planar or low-angle cross-stratified units with consistent orientation. Within the mudstone beds, shell fragments are present, but in the form of hash only. Coarse silts or very fine sand-sized siliciclastic material are sprinkled all over the facies, in both rock types. Quartz and feldspar are the major constituents of the siliciclastic fraction, while mica is virtually absent. Authigenic glauconite globules are common in both rock types. At places there are also very minute crystals of authigenic pyrite. Within the shell-rich component, the siliciclastic fraction is well-sorted and made up of fine-grained sand. The shells are much larger. The interstitial spaces between framework grains are filled by blocky ferroan calcite within the shelly beds and non-ferroan in the mudstone beds within each of the sedimentation units. The shells in this facies commonly retain their primary fabric and are dominantly made of non-ferroan calcite. Ferroan calcite, a very rare component, is confined within intercrystalline pores, with or without the skeletal grains.

The heavily weathered nature of the exposures prevents detailed assessment of the trace fossil assemblage. However, *Thalassinoides* are abundant (Figure 6h). Sponge borings are locally abundant.

Interpretation

The generally good sorting of the sub-rounded siliciclastic grains, combined with clear carbonate cement, indicates a high-energy depositional process. Abundant skeletal fragments, putatively having a calcitic mineralogy, suggest an open marine depositional setting. Trough cross-strata as internal structures are consistent with the high-energy shallow-shelf setting. The abundance of burrows points to a relatively low net rate of sedimentation. The thriving colonies of tubular rudist bivalves make the contention even more plausible. The presence of burrowed hard-grounds, at places, may be ascribed to early meteoric cementation (Knaust and Costamagna, 2012; Pérez-López and Pérez-Valera, 2012; Rameil *et al.*, 2012). Polygonal cracks suggest shallow-water deposition with occasional emergence above sea-surface at least temporally and locally. Non-ferroan clear blocky calcite cement supports this meteoric water influence, though not unequivocally (Grover and Read, 1983; Niemann and Read, 1988; Meyers, 1991). The absence of sand crystals, nonetheless, suggests that the dilution of sea water by fresh water was not as strong as it had been in the depositional sites of the previous two facies associations. The early cementation presumably encouraged growth of bioherms. Alternations between beds churned by burrowers and beds having few burrows, however, points to variable rates of sedimentation, possibly intervened by occasional storms. Apparently there were certain sheltered areas, probably behind the bioherms, not readily accessible to sediments and facies 4B formed as storm washover fans in such sheltered areas. The distinctly convex-up geometry of facies 4B is consistent with this depositional scheme; each unit, a shelly bed below and a mudstone bed above coupled together, presumably represents an individual event of storm deposition waning rapidly. In close spatial association with bioherms, the stratal geometry and graded beds in this facies readily support the depositional scenario envisaged for facies 4B.

Load casts manifesting temporally rapid sedimentation is perfectly consistent with the situation envisaged. Normal grading and common concave-up orientation of curved shells point to deposition from suspension. The low-angle cross-bedded layers are most likely the products of sediment accretion, but did not result from bedform migration. The calcite crystals among the framework elements in facies 4B, unlike those in facies 4A, are dirty, and depict perfect replacement of fine-grained matrix in agreement with the inferred depositional scenario. The compositional difference of calcite crystals in the groundmass between the two aforementioned bed components, ferroan in the lower shelly beds and non-ferroan in the upper muddy beds, is striking, but difficult to explain except if that the shelly beds got rapidly buried under impervious muddy beds cutting down oxygen supply.

4 Palaeocurrent

Widespread cross-strata and few ripples are the only traction structures amenable for depiction of the sediment dispersal pattern. The ripples are recognized exclusively within facies 1B and 3A. With straight or broadly sinuous crests, they are apparently wave generated (Figure 7). Although the lee orientation often reverses the crest orientation in these ripples highly consistently trends northeast-southwest. The cross-strata in facies 1A, despite having lesser consistency, have mean orientations at a high angle to wave ripple crests (Figure 2). Cross-bedded layers in facies 1B show clearly two opposite current directions, one roughly parallel and the other at a high angle to the cross-strata orientation noted in facies 1A. The former belongs to the sigmoidal cross-strata and the latter to the trough cross-strata.

In facies association 2, cross-strata are discernible in facies 2A only and they are unimodally oriented southeastwards. In facies 3A, the cross-strata orientation is in almost opposite direction. In facies 3B, it is almost bipolar, north-northwest−south-southeast. Eastward it is in facies 4A and north-northwestward in facies 4B, and unimodal in both cases.

5 Depositional model

As mentioned in the facies analysis, reconciliation between fossil and trace fossil occurrences, the sediment structures and textures, the occurrence of authigenic glauconite as well as the abundant presence of carbonates in

Figure 7 Wave ripple within the Garudamangalam Sandstone.

almost all facies constituents makes a marginal marine setting most likely for deposition of the Garudamangalam Sandstone. The consistent wave ripple crest orientation suggests a NE-SW alignment of the Ariyalur palaeoshoreline. Moreover, the to-and-fro tide movement, as recorded in facies 3B, is at a high angle to this direction. The accretion direction of the bay-mouth bar was evidently parallel to the palaeoshoreline presumably under wave influence (Coleman *et al.*, 1998; Shand *et al.*, 2001; Li *et al.*, 2011). Bearing a prominent fluvial signature, the bar represented by facies association 1, marine according to the fauna, most probably belonged to a river-dominated bird-foot delta. Deposition of facies association 2 took place in a mud-depositing low-energy bay environment that presumably had a connection with the sea, and that was positioned between the bay-mouth bar and the shoreline. On the other hand, facies association 4 with its well-sorted siliciclastic sands and open-marine fauna, is likely to have been deposited at a seaward side of the bar. Facies 4A apparently formed at the bar-fringe, where the generally high-energy conditions favoured the formation of rudist bioherms. The latter locally provided space to accommodate washover fans while storm waves spilled over them because of temporary piling up of sea water along the shore. Each bed, being shell-rich at the bottom and mud-rich at the top, represents a single storm event and the sedimentation in general was presumably intermittent.

The short vertical sections of the facies associations measured at different locations invariably show shoaling and an overall coarsening-upward trend (Figure 2). Bounded below by the shelf-originated Karai Shale Formation and above by an unconformity, the Garudamangalam Sandstone Formation is essentially a delta formed during highstand of the sea level (Tewari *et al.*, 1996; Watkinson *et al.*, 2007). The delta was apparently river-dominated. The depositional setting surrounding the southwestern wing of the modern Mississippi River bird-foot delta (Coleman *et al.*, 1998) is an analogue for the Cretaceous Garudamangalam Sandstone Formation. The narrow, elongated River Mississippi bar accretes in a shore-parallel direction under wave influence enclosing an embayment in the north and the open sea in the south; a tidal inlet pierces through the bar. The depositional model envisaged for the Cretaceous Garudamangalam Sandstone Formation is essentially the same, but with the sea on the east and patchy biogenic build-ups at the land-fringe (Figure 8).

6 Cathodoluminescence characteristics of carbonate components

The various carbonate components within the facies that constitute the Garudamangalam Sandstone Formation

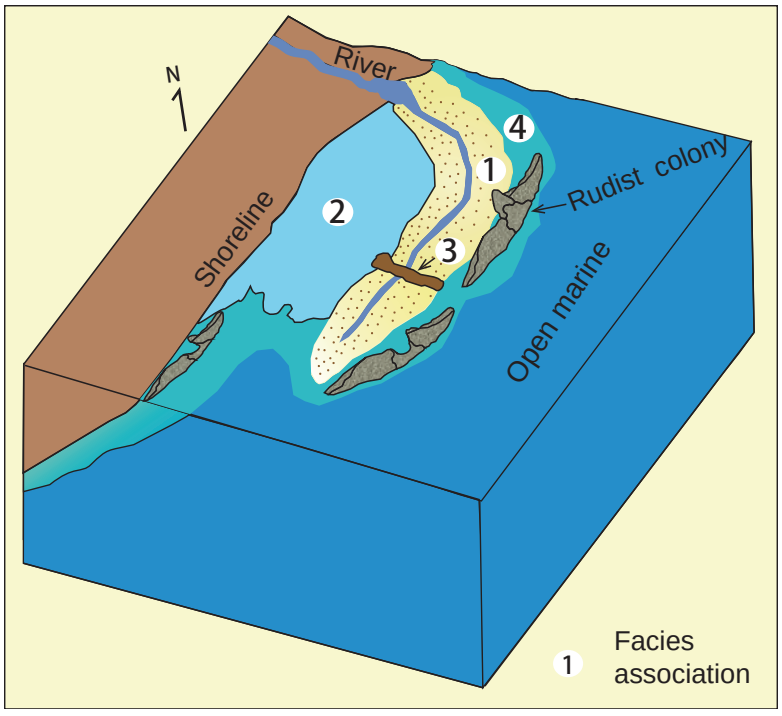

Figure 8 Depositional model for the Garudamangalam Sandstone Formation and distribution of its facies associations (1−4) (schematic, not to scale).

were tested for their cathodoluminescence (CL) characteristics. The purpose was to have a better idea about possible inhomogeneities in their composition, whether inherited or diagenetically acquired (Madden and Wilson, 2013). Model CL8200Mk5−2 of an optical cathodoluminescence system in the Sedimentology Laboratory of Jadavpur University, India, was used at 392−400 μA and 17.2 kV. Characteristics of the different components of the rocks are described and interpreted below (Figure 9).

Shells: In all facies, apart from the carbonate-free facies 1A, the shells which retained their primary fabric are generally non-luminescent, although some have thin interbands that are slightly luminescent. Exceptions occur where thin bands in accord with the primary fabric of

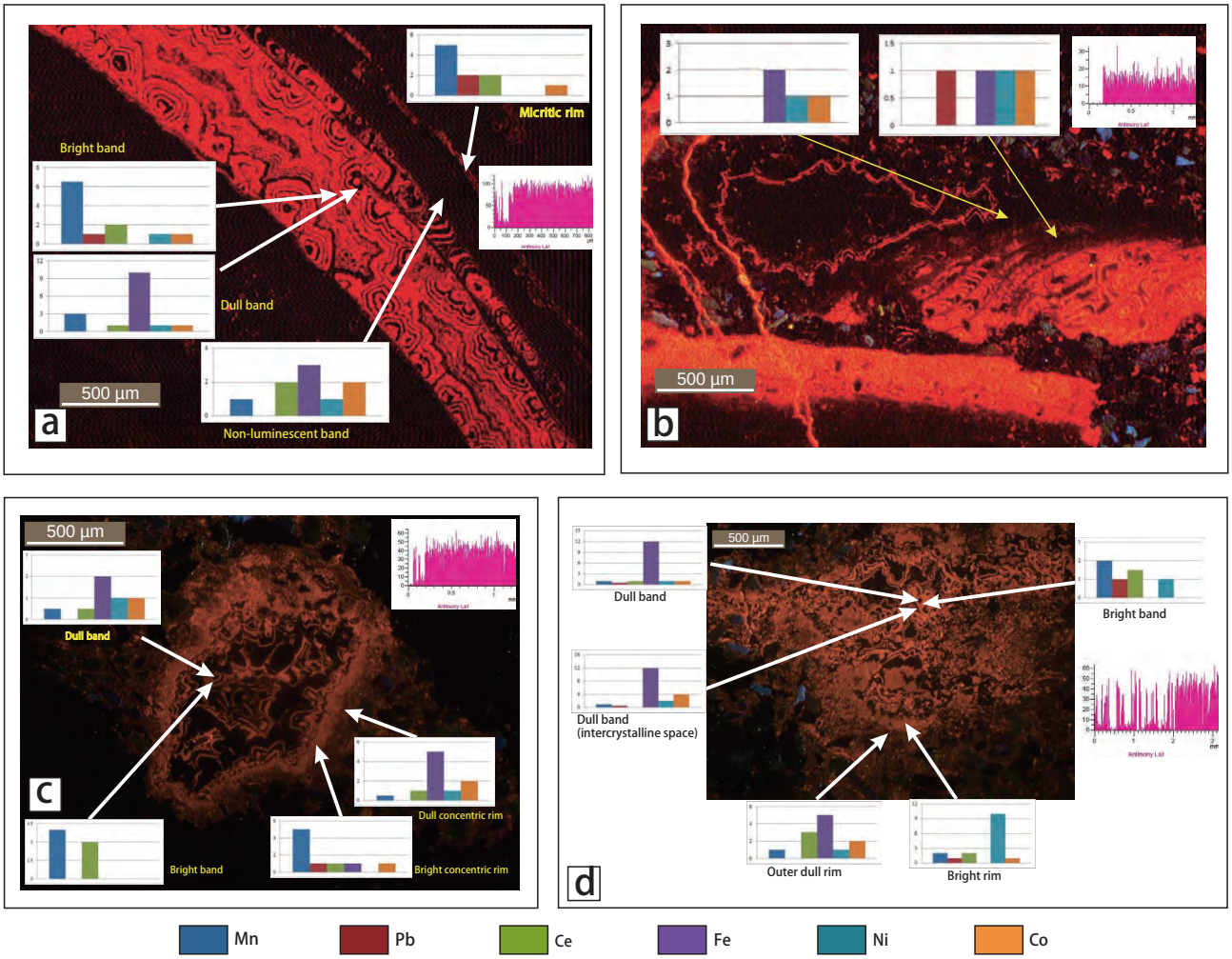

Figure 9 Cathodoluminescence of various carbonate components and compositional variations (histograms) in their different parts: a−A bivalve shell with preserved primary fabric; note that the sectorial zonation turns into a concentric zonation in the innermost part; also note the moderately luminescent micritized rim outside, followed inwards by a non-luminescent zone and then by alternating concentric zones of dull and bright lamellae resembling colloidal gel; further note the truncation of the lamellar bodies by growth lines of the shell and the generally high content of antimony (red curve); b−In this partially altered curved shell, the lower part shows bright orange luminescence, while the upper part is non-luminescent; the transition zone differs from the non-luminescent zone by having a significant quantity of Pb; note the large fluctuations in antimony content within the altered part; c−Pore-fill cement showing sectorial zonation giving way to concentric zonation inwards; the outer dull rim contains a significant quantity of Fe in contrast to the adjacent bright rim; in the case of concentric zonation, the bright lamellae are rich in Mn and Ce, while the dull lamellae are richer in Fe and other quenchers at their cost; d−In case of carbonate replacement of the groundmass within interstices among framework elements, it shows similar zonations as in the preceding case, implying that, among the two outer sectorial zonations, the dull zone is significantly enriched in Fe; in case of internal concentric zones, the dullness is attributable to a higher Fe content while the brightness is attributable to a high Mn and other sensitizers in absence of Fe. In contrast to the carbonate cement in the preceding case, these replacing carbonate groundmass has a strongly fluctuating antimony content.

shells show bright luminescence. Bright luminescence is also found in cements within intercrystalline pore spaces and dissolution voids (Brand *et al.*, 2012).

The shells in the first two figures apparently bear their original constituent crystals of stable minerals unaltered. Some bright growth bands presumably consisted of metastable minerals or were made of comparatively smaller crystals that underwent neomorphism in a less oxygenated diagenetic environment with Mn^{2+} without any significant suppression from Fe^{2+} abundance. It is safe to presume that intercrystalline pores and the dissolution voids were also filled up in a similar diagenetic setting.

***Micritic rims*:** The micritic rims around the shells are non-luminescent, irrespective of facies and irrespective of the fact that in one of the facies, facies 4A, they are exceptionally ferroan, at least in parts. Mn in quadrivalent state and Fe in ferric state on the sea floor were possibly responsible for this lack of luminescence. Similar non-luminescence even in the altered parts of the micritic rims suggests copious presence of Fe^{2+} in the diagenetic environment (Dromgoole and Walter, 1990; Machel *et al.*, 1991; Machel, 2000; Boggs Jr. and Krinsley, 2006).

***Moldic pores*:** Moldic pores always dominantly display bright luminescence; dull luminescence may, nevertheless, be present within intercrystalline spaces. The blocky calcite crystals filled the moldic pores in the lower part of the fresh-water vadose zone or in the top part of the fresh-water phreatic zone where the Mn^{2+}/Fe^{2+} ratio was positive (Machel, 2000; Rameil *et al.*, 2012). Subsequent migration of sediments to a greater depth could have reversed the ratio to generate dullness in the cement filling the spaces between the large crystals with bright illumination.

***Skeletal moldic pores and intraparticle pores*:** Within the skeletal moldic pores, concentric alternations between zones of dull or non-luminescent and bright illumination are characteristic. Concentric zonation is found also within intraparticle pores apparently without biogenic influence. The marked difference between the two cases is that, within skeletal material, the zonation is circular, growing all around, as it happens in the case of colloidal precipitation, whereas in pore-filling cement, the growth is unidirectional. Repeated changes in crystal growth rate, temperature or trace element partitioning are possibly a more likely explanation for these rapid illumination oscillations in concentric zones than changes in the redox potential of the pore water.

***Recrystallized or replaced groundmass*:** Blocky carbonate crystals either forming a groundmass as products of replacement or aggrading neomorphism show a mixed nature because of patchy alternations of bright and dull luminescence; the latter generally occupies the intercrystalline pores between the larger bright crystals. Away from the framework grains, possibly at the late stage of advancement of the recrystallization front, the zonation gives way to a zone of non-luminescence. The sectorial transition from an initially mixed luminescence to non-luminescence may in certain cases be superimposed by a few instances of concentric zonation. It is likely that neomorphism initiated in a dysoxic condition at the upper part of the fresh water phreatic zone, but continued in a deeper anoxic zone where an enhanced Fe^{2+} pressure suppressed the Mn^{2+} activity.

Fractures and fracture-induced veins: Carbonate cement-filling within fractures and putatively fracture-induced dissolution veins across both the framework elements and the groundmass show bright orange luminescence (Figure 10). The fractures are mostly hair-line and have mutually fitting boundaries in multiple straight segments; some are a little frayed. The dissolution veins are wider with mutually misfit and highly irregular walls cutting across clasts and groundmass with equal ease. The features are essentially of post-burial origin and their filling took place in a late diagenetic stage. The pore water from which the cement precipitated must have been rich in Mn in divalent state and there was not enough Fe^{2+} to suppress its activity.

7 Siliciclastic−carbonate mixing

A wide range of mixing processes of siliciclastic and carbonate components in the Garudamangalam Sandstone Formation becomes apparent now; some of them were in the depositional realm and others formed only in the diagenetic stage. Mixing took place in comparable extent within both realms; clear appraisal of the processes involved in both is a prerequisite for grasping the full significance of the mixing.

7.1 Depositional mixing

The entire depositional realm of the Cretaceous Garudamangalam Sandstone Formation witnessed mixing between siliciclastic and carbonate components in all the palaeogeographic sectors. Dwindling sand supply on the landward side of the bay-mouth bar allowed patchy growth of banks of calcium carbonate secreting biota in facies 2A. The process is essentially comparable to the "facies mixing" of Mount (1984). In facies 2B, the carbonate depositional component, whether skeletal or non-skeletal,

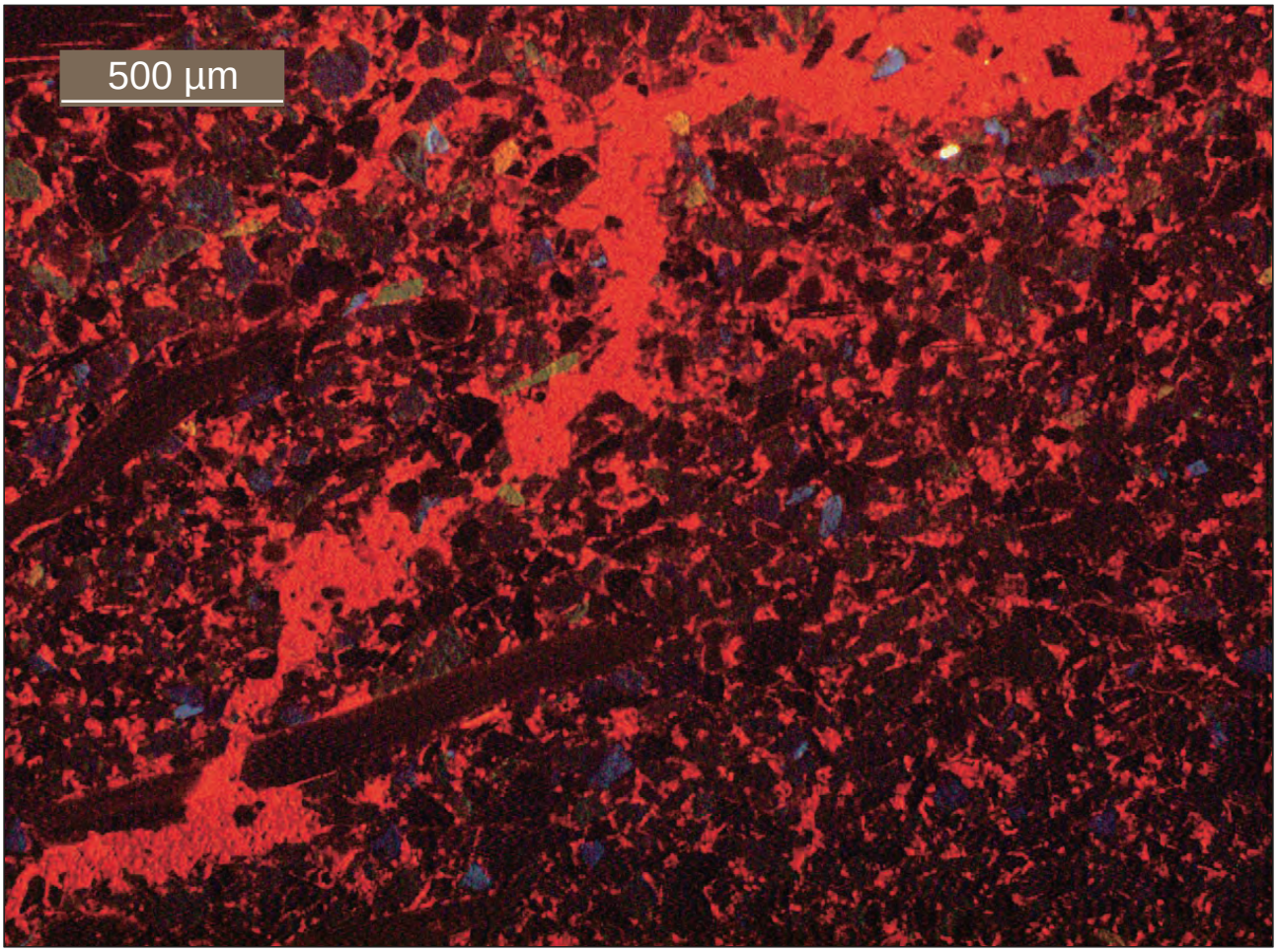

Figure 10 Carbonate-cement filling within fractures and fracture-induced dissolution veins.

is indigenous, while the siliciclastic component is not; the latter is obviously no hydraulic equivalent of the former.

In facies 3A, segregation of siliciclastic and carbonate depositional components was largely influenced by their respective hydraulic behaviour; a better buoyancy caused preferred concentration of carbonate clasts at the bedform toes; flow intensity variation had little effect. On the other hand, in the limestone component of facies 3B, segregation of bioclasts along the foreset bases is apparently related to repeated flow intensity fluctuations. In stark contrast, the deprivation of shells in the closely associated sandstone component of the same facies is likely related to a drop in supply. Such a development may arise from the emergence of shell banks because of sea level lowering or a diminishing biogenic production. To account for repeated vertical alternations between the limestone and sandstone components, one has to surmise either tidal cycles longer than the neap-spring cycles or biogenic cycles independent of sea level changes. Choice of the exact process is elusive at this stage.

In facies 4A, depositional mixing was limited, though it occurred, mainly due to the growth of bioherms of some rudists that were resistant enough to survive the prevailing siliciclastic influx. In facies 4B, the siliciclastic and carbonate components were supplied by the same current, but segregated during deposition because of size- and shape-dependent grain-settling behaviour.

7.2 Diagenetic mixing

The petrographic analyses show distinct compositional variations among the carbonate components of sediments; some are inherited and other ones diagenetic. In order to obtain a better insight into the extent and mode of introduction of diagenetic carbonates, an EDAX study was conducted on both biogenic and abiogenic components in correspondence to their CL characteristics. The EDAX facility available at Jadavpur University, Kolkata, has been utilized for the purpose. The Model INCA mics of the Inca Oxford Instruments was deployed and a 10 nm coating of palladium oxide was applied over the diamond-polished

thin sections. Though the investigation is still in its preliminary stage, some interesting results have already been obtained.

A chosen curved shell retaining its primary fabric displays both sectorial and concentric CL zonations. The micritic rim on the shell outer surface possesses a medium degree of luminescence; this is followed inwards by a thick non-luminescent band and then by a thicker band characterized by very thin concentric rings of alternating bright and dull luminescence (Figure 9a). The completely enclosing rings in the innermost band give an impression of precipitation from a colloidal gel. The rings are found to end abruptly against some laterally impersistent shell-growth lines, attesting their primary origin. Histograms associated with this figure depict the average compositional variations between rings of contrasting CL characters; those elements known to control the CL character are preferentially considered (Machel, 1983, 1984; Machel *et al.*, 1991). The bright rings apparently owe their CL character to the abundance of Mn, presumably in bivalent state, having also Pb and Ce as additional sensitizers; little iron is there to counter them, although some amounts of nickel and cobalt are present as luminescence quenchers. Contrastingly the dull rings alternating with them have a clearly reduced content of Mn and Pb but are rich in iron, presumably again in bivalent state. Although Major (1991) asserted that cathodoluminescence in carbonates is diagenetic, Grossman *et al.* (1996) recognized intrashell variations like this as seasonal. These nano-scale variations in the presence of larger-scale intrashell sectorial variations, nevertheless, point to a much smaller scale of variations in the biotic life cycle, most probably driven by day-night variations in crystal growth rate. Significant variations in the coral growth rate in response to experimentally-driven alterations in illumination, as Howe and Marshall (2002) recorded, strongly support this contention. The dependence of trace element partitioning on crystal growth rate is well established (*e.g.*, Lorens, 1981; Mucci and Morse, 1983; Pingitore Jr. and Eastman, 1986; Dromgoole and Walter, 1990; Schmidt *et al.*, 2008). The middle band is as non-luminescent CL as is usually expected in unaltered marine shells (Meyers, 1974; Pierson, 1981). The compositional histogram records the dominance of quenchers like Fe, Ni and Co over sensitizers like Mn and Ce. The sectorial change from the inner band may record a transition from a warmer to a cooler phase in the life cycle (Howe and Marshall, 2002), significantly altering the crystal growth rate and consequently the metal ion partitioning. An alternative could be partial diagenesis in the non-luminescent band, but strict fabric-selectivity makes this alternative unlikely. Maintenance of a similarly enhanced content of antimony across the boundary of the two bands of contrasting CL characters supports the contention, and further asserts that both bands have retained their primary characters (Figure 9a). The micritic rim, of putative sea-floor origin, on the outer surface of the shell is, however, an unambiguous product of diagenesis possibly earning its present moderate CL luminescence through multiple phases of alteration. The moderate amount of Mn^{2+} and other sensitizers like Pb and Ce in the scarce presence of quenchers contributed CL character (Liu *et al.*, 1988).

Another curved shell was chosen for being non-luminescent where it is altered in contrast to its brightly luminescent unaltered part (Figure 9b). The contact between the two parts of contrasting CL characteristics is irregular and fuzzy. EDAX of the altered non-luminescent part displays the similar, generally high antimony content, but neither as high nor as uniform as in the previous example. Significantly, quenchers like Fe, Ni and Co dominate in the non-luminescent zone, but Pb dominates over them in the zone transitional to bright luminescence. Apparently the pore water that became enriched in antimony on dissolution of the shell, enhanced the antimony content within the crystals that precipitated from it; the uptake amount, nonetheless, varied because of variations in crystal growth rate not resolvable in CL characteristics.

A dissolution pore-fill of unambiguous diagenetic origin displays sectorial alterations followed inwards by concentric alternations in CL character; the concentric alternations in this case, however, depict unidirectional inward growth of rhombic crystals unlike those in the preceding biotic entity (Figure 9c). The thin outer rim of fibrous needle-shaped crystals having dull CL contains a substantial proportion of Fe, while the immediately following thick bright band yields a substantial enhancement in sensitizers like Mn and Ce at the cost of the quenchers, including Fe (Figure 9c). Unlike the first case with the biotic example, the transition between the two bands of contrasting CL characters is gradational and prompts the suggestion that it took place under the command of progressively decreasing ionic concentration in water confined within the pores and consequently reducing the crystal growth rate. In the case of concentric alternations filling the rest of the pore space, the composition of the bright lamellae shows an obvious enrichment in sensitizers, especially Mn and Ce, as in case of sectorial variation and the dull lamellae alternating with them have a predominance of quenchers, especially Fe (Figure 9c). The sharp alternations in CL characteristics in

this confined pore space may be attributed to salinity fluctuations. Alternatively, fluctuations in activity of sulphur-reducing bacteria may be responsible; enhanced bacterial activity locking Fe into pyrite could have contributed to the bright CL.

The carbonate mass replacing the primary matrix among the framework grains shows changes that are roughly similar to the dissolution pore-filling cement, possibly because under sedimentary physicochemical conditions, replacement can run only through the same solution-precipitation pathway. The replacement presumably initiated from grain-margins that are most permeable for the solution. Consequently, the initial sectorial zonation gave way to a concentric zonation as the replacement front advanced. The outer dull rim owes its CL character to the much higher proportion of Fe with respect to Mn, the latter being at least in bivalent state. The histogram is largely similar that for the filling within the studied dissolution voids. The next rim inwards with bright CL is, nevertheless, different for the two cases; in this replacement product , the Ni content is high, although Fe is totally absent. The bright CL, despite the considerably high Ni content, once more confirms the fact that the Mn^{2+}/Fe^{2+} ratio has more control on the CL character than the trace element contents (Machel, 2000; Boggs Jr. and Krinsley, 2006). In the next inward band of the concentric zonation, the dull CL is attributable to a high Fe content and the bright CL to a high Mn content, although the contents of Ce and Pb in fairly good amount augmented the brightness. The intrasectorial nanometric alternations in the last band might have been driven by a fluctuating pH of the pore water controlling carbonate crystal growth rate and consequently the trace element partitioning (Terakado and Taniguchi, 2006). The crystal growth rate variation also explains the very wide variation in Sb content within these replacement carbonates (Figure 9d).

8 Conclusions

The Cretaceous Garudamangalam Sandstone Formation at Ariyalur, India, a highstand systems tract, unveils a wide range of siliciclastic−carbonate mixing modes in a nearshore marine realm associated with a river-mouth bar. Although deposition took place in a narrow belt, palaeoenvironmental conditions differed widely. The presence of a shore-parallel river-mouth bar resulted in a restricted environment on its shoreward side, while its seaward side remained open marine. A connection between the two contrasting energy regimes was maintained by one or more tidal inlets. The shoreline alignment being almost north-south, the marked energy contrast was most outspoken in a roughly east-west transect.

The mixing modes can be divided into two categories, *viz.* depositional and diagenetic. In both categories the mixing modes are biogenic as well as abiogenic. The most common mode of mixing is at the transition between two laterally adjacent facies of contrasting compositions. In any natural setting, the contact between two indigenous facies is always blurred because of mixing of their constituents and does not merit search for any other tortuous explanation for the mixing. Patchy build-ups of colonies of calcium carbonate secreting organisms within siliciclastic depositional settings may not be favoured, but are not uncommon either. Isolated mesoscale patches of rudist colonies and microscale mounds of red algae within sandstones are examples. Mixing also took place when silt-sized dust settled from the air onto an indigenous carbonate mudflat. An admixture of siliceous and carbonate clastics often arose because of simultaneous transport of both components by the same current. Different settling behaviours, however, generally segregated the two components in two different parts of the beds. Preferred accumulations of carbonate shells at the bottom of the beds both as traction and as suspended loads in the facies associations 3 and 4 respectively are examples apt enough. Alternate sandstone and shell-rich limestone beds, as observed in facies association 3, may result from interfingering between two contemporary facies deposited in spatially apart contrasting energy spectra or from temporal variability in carbonate productivity.

Spectral variation in diagenetic mixing can, indeed, be comparable with that of depositional mixing. The most common is perhaps preferred replacement of finer-grained matrix by carbonate within siliciclastic sediments. The replacement is likely to initiate at grain margins, most readily penetrable to the replacing solution. During further progress of the replacing front into the grain interstices, the solution may undergo compositional transformation. Although a fine-grained matrix is preferred, replacement has affected the framework of siliciclastic grains too. Carbonate filling within intraparticle pores and dissolution cavities also led to diagenetic mixing. Filling of dissolution cavities within and without shells may not be entirely abiogenic. Another common mode of diagenetic mixing arises from carbonate cement filling veins. The rapidly changeable carbonate components, inherited or acquired, add a different dimension to the compositional mixing through subsequent alterations. The micritic rims on shells

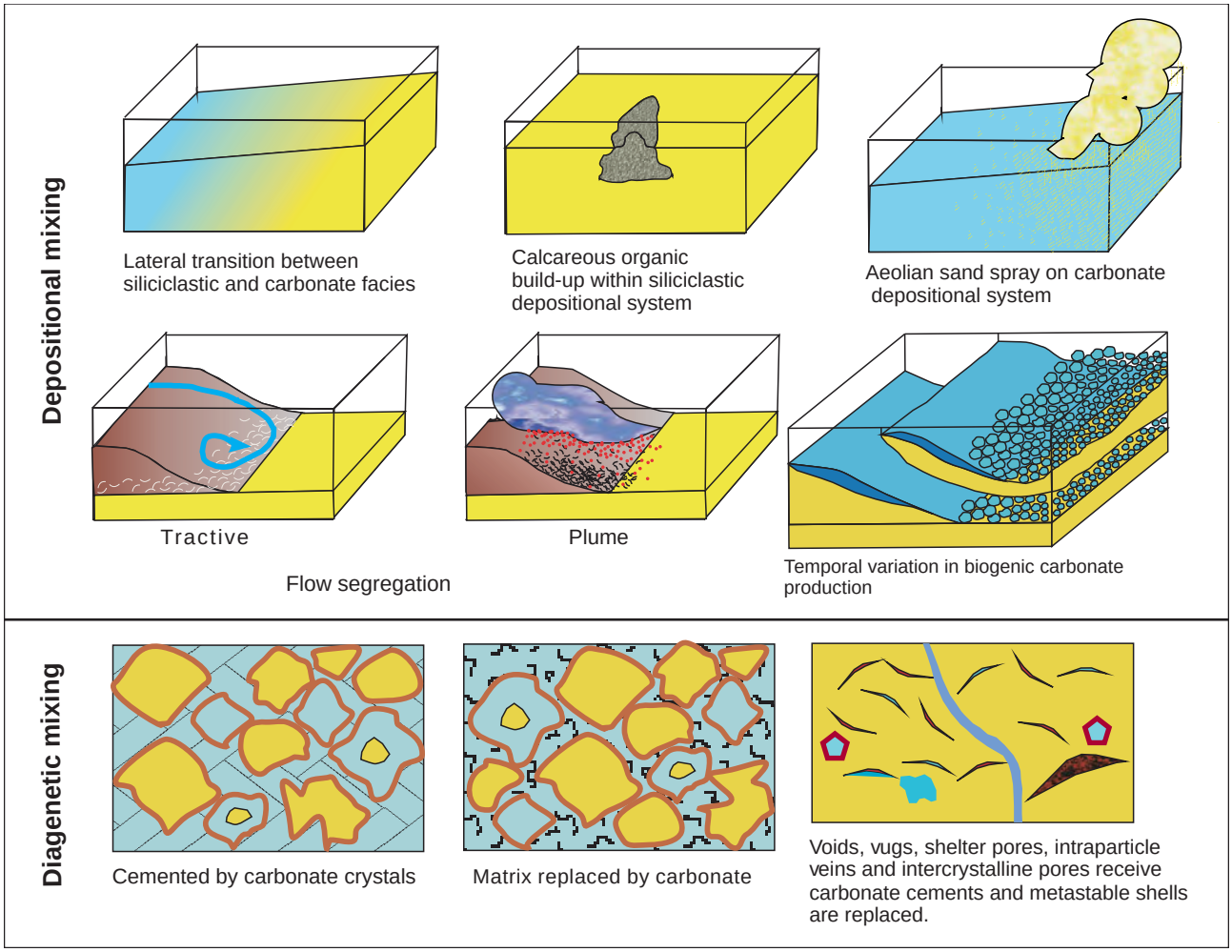

Figure 11 Possible modes of depositional and diagenetic mixing of siliciclastic and carbonate sediments.

constitute a common example.

Because of the finer grain size, their constituent crystals are prone to further alteration in composition during successive stages of diagenesis. Though originating primarily from biogenic activity, this feature may ultimately acquire a composition controlled by non-biogenic processes. The shell composition may be inherently variable. Further variability is induced through partial dissolution and later filling of the resulting cavities. The carbonate cement filling of skeletal moldic pores has a composition quite different from the primary composition of the shell. In fine tune, the carbonate components of a rock may differ significantly amongst themselves, adding further intricacy to the compositional mixing (Figure 11). Variability in crystal growth rate, temperature, salinity, redox potential, pore-water composition and biogenic influence, especially of microbiota comes into play. On the long term, the carbonate components acquire strongly variable compositions, especially in trace element content; they highlight the need for extensive geochemical exploration if a better insight is to be obtained.

Acknowledgements

The authors gratefully thank the two anonymous reviewers for their constructive suggestions and criticisms. Subir Sarkar acknowledges the CAS (Phase V) and UPE II programmes of Jadavpur University. Nivedita Chakraborty and Anudeb Mandal acknowledge UGC and CSIR respectively for their financial support. The Department of Geological Sciences, Jadavpur University provided infrastructural help.

References

Ayyasami, K., Banerji, R. K., 1984. Cenomanian-Turonian transition in the Cretaceous of southern India. Bulletin of the Geological Society of Denmark, 33(1): 21−30.

Bathurst, R. G. C., 1975. Carbonate Sediments and Their Diagenesis (2nd Edition). Developments in Sedimentology 12. Amsterdam: Elsevier, 1−658.

Belperio, A. P., Searle, D. E., 1988. Terrigenous and carbonate sedimentation in the Great Barrier Reef province. In: Doyle, L. J., Roberts, H. H., (eds). Carbonate-Clastic Transitions. Developments in Sedimentology 42. Amsterdam: Elsevier, 143−174.

Blanford, H. F., 1862. On the Cretaceous and other rocks of the South Arcot and Trichinopoly Districts, Madras. Memoirs of the Geological Survey of India, 4(1): 1−217.

Boggs Jr., S., Krinsley, D., 2006. Application of Cathodoluminescence Imaging to the Study of Sedimentary Rocks. New York: Cambridge University Press, 1−165.

Brand, U., Jiang, G. Q., Azmy, K., Bishop, J., Montañez, I P., 2012. Diagenetic evaluation of a Pennsylvanian carbonate succession (Bird Spring Formation, Arrow Canyon, Nevada, U.S.A.) — 1: Brachiopod and whole rock comparison. Chemical Geology, 308−309: 26−39.

Buatois, L. A., Mángano, M. G., 2011. Ichnology: Organism-Substrate Interactions in Space and Time. Cambridge: Cambridge University Press, 1−358.

Cant, D. J., Walker, R. G., 1978. Fluvial processes and facies sequences in the sandy braided South Saskatchewan River, Canada. Sedimentology, 25(5): 625−648.

Chaudhuri, A., Howard, J. D., 1985. Ramgundam Sandstone: A Middle Proterozoic shoal-bar sequence. Journal of Sedimentary Petrology, 55(3): 392−397.

Choquette, P. W., James, N. P., 1987. Diagenesis #12. Diagenesis in Limestones − 3. The Deep Burial Environment. Geoscience Canada, 14(1): 3−35.

Coleman, J. M., Roberts, H. H., Stone, G. W., 1998. Mississippi River Delta: An overview. Journal of Coastal Research, 14(3): 699−716.

Cornée, J. J., Léticée, J. L., Münch, P., Quillévéré, F., Lebrun, J. F., Moissette, P., Braga, J. C., Melinte-Dobrinescu, M., De Min, L., Oudet, J., Randrianasolo, A., 2012. Sedimentology, palaeoenvironments and biostratigraphy of the Pliocene−Pleistocene carbonate platform of Grande-Terre (Guadeloupe, Lesser Antilles forearc). Sedimentology, 59(5): 1426−1451.

Dromgoole, E. L., Walter, L. M., 1990. Iron and manganese incorporation into calcite: Effects of growth kinetics, temperature and solution chemistry. Chemical Geology, 81(4): 311−336.

Dunbar, G. B., Dickens, G. R., 2003. Late Quaternary shedding of shallow-marine carbonate along a tropical mixed siliciclastic-carbonate shelf: Great Barrier Reef, Australia. Sedimentology, 50(6): 1061−1077.

Dworschak, P. C., Rodrigues, S. de A., 1997. A modern analogue for the trace fossil *Gyrolithes*: Burrows of the thalassinidean shrimp *Axianassa australis.* Lethaia, 30(1): 41−52.

Fielding, C. R., 1986. Fluvial channel and overbank deposits from the Westphalian of the Durham coalfield, NE England. Sedimentology, 33(1): 119−140.

Folk, R. L., Andrews, P. B., Lewis, D. W., 1970. Detrital sedimentary rock classification and nomenclature for use in New Zealand. New Zealand Journal of Geology and Geophysics, 13(4): 937−968.

Gibling, M. R., 2006. Width and thickness of fluvial channel bodies and valley fills in the geological record: A literature compilation and classification. Journal of Sedimentary Research, 76(5): 731−770.

Gingras M. K., MacEachern, J. A., Dashtgard, S. E., 2012. The potential of trace fossils as tidal indicators in bays and estuaries. Sedimentary Geology, 279: 97−106.

Govindan, A., Ravindran, C. N., Rangaraju, M. K., 1996. Cretaceous stratigraphy and planktonic foraminiferal zonation of Cauvery Basin, South India. Memoirs of the Geological Society of India, 37: 155−187.

Govindan, A., Yadagiri, K., Ravindran, C. N., Kalyanasundar, R., 1998. A Field Guide on Cretaceous Sequences of Trichinopoly Area, Cauvery Basin, India. Chennai: Oil and Natural Gas Corporation Limited, 1−53.

Grossman, E. L., Mii, H. S., Zhang C. L., Yancey T. E., 1996. Chemical variation in Pennsylvanian brachiopod shells: Diagenetic, taxonomic, microstructural, and seasonal effects. Journal of Sedimentary Research, 66(5): 1011−1022.

Grover, G., Read, J. F., 1983. Paleoaquifer and deep burial related cements defined by regional cathodoluminescent patterns, Middle Ordovician carbonates, Virginia. AAPG Bulletin, 67(8): 1275−1303.

Hart, M. B., Tewari, A. T., Watkinson, M. P., 1996. Wood borings from the Trichinopoly Sandstone of the Cauvery Basin, South-East India. In: Pandey, J., Azmi, R. J., Bhandari, A., Dave, A., (eds). Contributions to XV Indian Colloquium on Micropaleontology and Stratigraphy. Dehra Dun: The K. D. Malaviya Institute of Petroleum Exploration and the Wadia Institute of Himalayan Geology, 529−539.

Holmes, C. W., Evans, R. G., 1963. Sedimentology of Gullivan Bay and vicinity, Florida. Sedimentology, 2(3): 189−206.

Howe, S. A., Marshall, A. T., 2002. Temperature effects on calcification rate and skeletal deposition in the temperate coral, *Plesiastrea versipora* (Lamarck). Journal of Experimental Marine Biology and Ecology, 275(1): 63−81.

Kale, A. S., Lotfalikani, A., Phansalkar, V. G., 2000. Calcareous nanofossils from the Uttatur group of Trichinopoly Cretaceous, South India. In: Govindan, A., (ed). Cretaceous Stratigraphy—An Update. Memoirs of the Geological Society of India, 46: 213−227.

Kaufmann, B., 1997. Diagenesis of Middle Devonian carbonate mounds of the Mader Basin (eastern Anti-Atlas, Morocco). Journal of Sedimentary Research, 67(5): 945−956.

Kidwell, S. M., 1991. Taphonomic feedback (live/dead interactions) in the genesis of bioclastic beds: Keys to reconstructing sedimentary dynamics. In: Einsele, G., Ricken, W., Seilacher, A., (eds). Cycles and Events in Stratigraphy. Berlin: Springer-Verlag, 268−280.

Knaust, D., Costamagna, L. G., 2012. Ichnology and sedimentology

of the Triassic carbonates of North-west Sardinia, Italy. Sedimentology, 59(4): 1190−1207.

Larcombe, P., Woolfe, K. J., 1999. Terrigenous sediments as influences upon Holocene nearshore coral reefs, central Great Barrier Reef, Australia. Australian Journal of Earth Science, 46(1): 141−154.

Larsonneur, C., Bouyssee, P., Auffret, J., 1982. The superficial sediments of the English Channel and its western approaches. Sedimentology, 29(6): 851−864.

Li, W. G., Bhattacharya, J. P., Zhu, Y. J., Garza, D., Blankenship, E., 2011. Evaluating delta asymmetry using three-dimensional facies architecture and ichnological analysis, Ferron 'Notom Delta', Capital Reef, Utah, USA. Sedimentology, 58(2): 478−507.

Liu, Y. G., Miah, M. R. U., Schmitt, R. A., 1988. Cerium: A chemical tracer for paleo-oceanic redox conditions. Geochimica et Cosmochimica Acta, 52(6): 1361−1371.

Longhitano, S. G., Nemec, W., 2005. Statistical analysis of bed-thickness variation in a Tortonian succession of biocalcarenitic tidal dunes, Amantea Basin, Calabria, southern Italy. Sedimentary Geology, 179(3−4): 195−224.

Lorens, R. B., 1981. Sr, Cd, Mn and Co distribution coefficients in calcite as a function of calcite precipitation rate. Geochimica et Cosmochimica Acta, 45(4): 553−561.

Machel, H. G., 1983. Facies and diagenesis of some Nisku buildups and associated strata, Upper Devonian, Alberta, Canada. In: Harris, P. M., (ed). Carbonate Buildups. SEPM Core Workshop Notes, 4: 144−181.

Machel, H. G., 1984. Facies and dolomitization of the Upper Devonian Nisku Formation in the Brazeau, Pembina, and Bigoray areas, Alberta, Canada. In: Eliuk, L., (ed). Carbonates in Subsurface and Outcrop. 1984 CSPG Core Conference, 191−224.

Machel, H. G., 2000. Application of cathodoluminescence to carbonate diagenesis. In: Pagel, M., Barbin, V., Blanc, P., Ohnenstetter, D., (eds). Cathodoluminescence in Geosciences. Berlin: Springer-Verlag, 271−301.

Machel, H. G., Mason, R. A., Mariano, A. N., Mucci, A., 1991. Causes and emission of luminescence in calcite and dolomite. In: Barker, C. E., Kopp, O. C., (eds). Luminescence Microscopy and Spectroscopy: Qualitative and Quantitative Applications. SEPM Short Course Notes, 25: 9−25.

Madden, R. H. C., Wilson, M. E. J., 2013. Diagenesis of a SE Asian Cenozoic carbonate platform margin and its adjacent basinal deposits. Sedimentary Geology, 286−287: 20−38.

Major, R. P., 1991. Cathodoluminescence in Post-Miocene carbonates. In: Barker, C. E., Kopp, O. C., (eds). Luminescence Microscopy and Spectroscopy: Qualitative and Quantitative Applications. SEPM Short Course Notes, 25: 149−153.

Meyers, W. J., 1974. Carbonate cement stratigraphy of the Lake Valley Formation (Mississippian), Scaramento Mountains, New Mexico. Journal of Sedimentary Petrology, 44(3): 837−861.

Meyers, W. J., 1991. Calcite cement stratigraphy: An overview. In: Barker, C. E., Kopp, O. C., (eds). Luminescence Microscopy and Spectroscopy: Qualitative and Quantitative Applications. SEPM Short Course Notes, 25: 133−148.

Miall, A. D., 1996. The Geology of Fluvial Deposits: Sedimentary Facies, Basin Analysis and Petroleum Geology. Berlin: Springer-Verlag, 1−582.

Morse, J. W., Mackenzie, F. T., 1990. Geochemistry of Sedimentary Carbonates. Developments in Sedimentology 48. Amsterdam: Elsevier, 1−707.

Mount, J. F., 1984. Mixing of siliciclastic and carbonate sediments in shallow shelf environments. Geology, 12(7): 432−435.

Mucci, A., Morse, J. W., 1983. The incorporation of Mg^{2+} and Sr^{2+} into calcite overgrowths: Influences of growth rate and solution composition. Geochimica et Cosmochimica Acta, 47(2): 217−233.

Nagendra, R., Kamalak Kannan, B. V., Sen, G., Gilbert, H., Bakkiaraj, D., Reddy, A. N., Jaiprakash, B. C., 2011. Sequence surfaces and paleobathymetric trends in Albian to Maastrichtian sediments of Ariyalur area, Cauvery Basin, India. Marine and Petroleum Geology, 28(4): 895−905.

Nagendra, R., Patel, S. J., Deepankar, R., Reddy, A. N., 2010. Bathymetric significance of the ichnofossil assemblages of the Kulakkalnattam Sandstone, Ariyalur area, Cauvery Basin. Journal of the Geological Society of India, 76(5): 525−532.

Niemann, J. C., Read, J. F., 1988. Regional cementation from unconformity-recharged aquifer and burial fluids, Mississippian Newman Limestone, Kentucky. Journal of Sedimentary Petrology, 58(4): 688−705.

Pearson, N. J., Gingras, M. K., 2006. An ichnological and sedimentological facies model for muddy point-bar deposits. Journal of Sedimentary Research, 76(5): 771−782.

Pérez-López, A., Pérez-Valera, F., 2012. Tempestite facies models for the epicontinental Triassic carbonates of the Betic Cordillera (southern Spain). Sedimentology, 59(2): 646−678.

Pettijohn, F. J., 1975. Sedimentary Rocks (3rd Edition). New York: Harper and Row, 1−628.

Pierson, B. J., 1981. The control of cathodoluminescence in dolomite by iron and manganese. Sedimentology, 28(5): 601−610.

Pingitore Jr., N. E., Eastman, M. P., 1986. The coprecipitation of Sr^{2+} with calcite at 25 °C and 1 atm. Geochimica et Cosmochimica Acta, 50(10): 2195−2203.

Pirrie, D., Ditchfield, P. W., Marshall, J. D., 1994. Burial diagenesis and pore-fluid evolution in a Mesozoic back-arc basin: The Marambio Group, Vega Island, Antarctica. Journal of Sedimentary Research, 64(3a): 541−552.

Ramasamy, S., Banerji, R. K., 1991. Geology, petrography and systematic stratigraphy of the pre-Ariyalur sequence in Trichinopoly district, Tamil Nadu, India. Journal of the Geological Society of India, 37: 577−594.

Rameil, N., Immenhauser, A., Csoma, A. É. and Warrlich, G., 2012. Surfaces with a long history: The Aptian top Shu'aiba Formation unconformity, Sultanate of Oman. Sedimentology, 59(1): 212−248.

Ramkumar, M., Stüben, D., Berner, Z., 2004. Lithostratigraphy,

depositional history and sea level changes of the Cauvery Basin, southern India. Annales Géologiques de la Péninsule Balkanique, 65: 1−27.

Ryan-Mishkin, K., Walsh, J. P., Corbett, D. R., Dail, M. B., Nittrouer, J. A., 2009. Modern sedimentation in a mixed siliciclastic-carbonate coral reel environment, La Parguera, Puerto Rico. Caribbean Journal of Science, 45(2−3): 151−167.

Sastry, M. V. A., Rao, B. R. J., Mamgian, V. D., 1968. Biostratigraphic zonation of the Upper Cretaceous formations of the Trichinopoly district, South India. Memoirs of the Geological Society of India, 2: 10−17.

Schmidt, D. N., Elliott, T., Kasemann, S. A., 2008. The influences of growth rates on planktic foraminifers as proxies for palaeostudies — A review. Geological Society, London, Special Publications, 303: 73−85.

Shand, R. D., Bailey, D. G., Shepherd, M. J., 2001. Longshore realignment of shore-parallel sand-bars at Wanganui, New Zealand. Marine Geology, 179(3−4): 147−161.

Sundaram, R., Henderson, R. A., Ayyasami, K., Stilwell, J. D., 2001. A lithostratigraphic revision and palaeoenvironmental assessment of the Cretaceous System exposed in the onshore Cauvery Basin, southern India. Cretaceous Research, 22(6): 743−762.

Terakado, Y., Taniguchi, M. 2006. A new method for the study of trace element partitioning between calcium carbonate and aqueous solution: A test case for Sr and Ba incorporation into calcite. Geochemical Journal, 40(2): 161−170.

Terwindt, J. H. J., 1988. Palaeo-tidal reconstructions of inshore tidal depositional environments. In: de Boer, P. L., van Gelder, A., Nio, S. D., (eds). Tide-Influenced Sedimentary Environments and Facies. Dordrecht: D. Reidel Publishing Company, 233−263.

Tewari, A., Hart, M. B., Watkinson, M. P., 1996. A revised lithostratigraphical classification of the Cretaceous rocks of Trichinopoly District, Cauvery Basin, Southeast India. In: Pandey, J., Azmi, R. J., Bhandari, A., Dave, A., (eds). Contributions to XV Indian Colloquium on Micropaleontology and Stratigraphy. Dehra Dun: The K. D. Malaviya Institute of Petroleum Exploration and the Wadia Institute of Himalayan Geology, 789−800.

Tewari, A., Hart, M. B., Watkinson, M. P., 1998. Teredolites from the Garudamangalam Sandstone Formation (Late Turonian-Coniacian), Cauvery Basin, Southeast India. Ichnos, 6(1−2): 75−98.

Tucker, M. E., 1981. Sedimentary Petrology: An Introduction. Oxford: Blackwell Scientific Publications, 1−252.

van Heerden, I. L., Roberts, H. H., 1988. Facies development of Atchafalaya Delta, Louisiana: A modern bayhead delta. AAPG Bulletin, 72(4): 439−453.

Watkinson, M. P., Hart, M. B., Joshi, A., 2007. Cretaceous tectonostratigraphy and the development of the Cauvery Basin, Southeast India. Petroleum Geoscience, 13(2): 181−191.

Wright, E. E., Hine, A. C., Goodbred Jr., S. L., Locker S. D., 2005. The effect of sea-level and climate change on the development of a mixed siliciclastic-carbonate, deltaic coastline: Suwannee River, Florida, U.S.A. Journal of Sedimentary Research, 75(4): 621−635.

(Edited by Xiu-Fang Hu)